

N63-19279

NASA TN D-1945



TECHNICAL NOTE

D-1945

THE COUPLED DYNAMIC RESPONSE OF A
TANK PARTIALLY FILLED WITH A LIQUID AND UNDERGOING FREE
AND FORCED PLANAR OSCILLATIONS

By David G. Stephens and H. Wayne Leonard

Langley Research Center
Langley Station, Hampton, Va.

REPRODUCED BY
NATIONAL TECHNICAL
INFORMATION SERVICE
U. S. DEPARTMENT OF COMMERCE
SPRINGFIELD, VA. 22161

NATIONAL AERONAUTICS AND SPACE ADMINISTRATION
WASHINGTON

August 1963

NATIONAL AERONAUTICS AND SPACE ADMINISTRATION

TECHNICAL NOTE D-1945

THE COUPLED DYNAMIC RESPONSE OF A
TANK PARTIALLY FILLED WITH A LIQUID AND UNDERGOING FREE
AND FORCED PLANAR OSCILLATIONS*

By David G. Stephens and H. Wayne Leonard

SUMMARY

An analytical and experimental investigation was conducted to determine the coupled dynamic response of a liquid-tank combination undergoing free and forced planar oscillations. The experimental portion of the investigation was conducted by using a partially filled cylindrical tank fitted with baffles and suspended to allow freedom in pitch and translation. An excitation force was provided by a small air jet coupled to the base of the tank. Experimental data are presented to show the effects of liquid damping, excitation force, and coupled natural frequency on the stability of the system. Analytical results, obtained by use of the pendulum analogy to simulate the dynamic characteristics of the liquid, are also presented. Comparisons of the analytical results with those obtained experimentally indicate that the pendulum analogy provides a very effective method for the determination of coupled natural frequencies of partially filled tanks undergoing planar translatory and pitching oscillations.

The data further indicate that the pendulum analogy yields valid modal damping for systems in which the tank experiences purely translatory motions if the pendulum is damped so that its decrement is equal to the decrement of liquid amplitudes in an identical static tank fitted with the same baffle configuration. The pendulum analogy, incorporating these damping values, will not, however, yield valid modal damping for the same system undergoing pitching oscillations. This apparent discrepancy may be attributed to a basic difference in the behavior of the liquid, and hence, a difference in the liquid damping, which was found to exist between translating and pitching systems. Limited data on the damping of a pitching tank containing a liquid are presented to illustrate this difference.

*The information presented herein is based in part upon a thesis entitled "An Analytical and Experimental Investigation of the Stability of an Analogous Liquid Propellant Space Vehicle" submitted by David G. Stephens in partial fulfillment of the requirements for the degree of Master of Science in Engineering Mechanics, Virginia Polytechnic Institute, Blacksburg, Virginia, May 1963.

INTRODUCTION

During the past few years, considerable research has been conducted on the dynamics associated with the sloshing of liquids in missile and space vehicles. The primary objectives of this research were to define the basic phenomena associated with the liquid motion and to determine the effects of this motion on the dynamic stability of liquid-carrying vehicles. Guidelines for much of the work were set forth by problems encountered in early vehicles. Observations of vehicle flights were sufficient to define the elemental sources of sloshing instabilities and to suggest areas where immediate basic research was required.

It was observed that in any rocket flight, the vehicle body is subjected to translatory and pitching perturbations from such external sources as guidance and control inputs and horizontal-wind shears. Vehicle body motions of this type result in disturbances of the contained liquid. If the perturbations occur at a frequency near that of the fundamental antisymmetric liquid mode, the liquid is forced to oscillate at amplitudes sufficiently large to produce severe destabilizing forces and moments on the vehicle (ref. 1). The severity of this destabilizing influence is cited in reference 2, where the failure of large boost vehicles has been attributed to fuel sloshing. The relative magnitude of the liquid oscillation is highly dependent upon and may therefore be controlled by the damping applied to the liquid by baffles placed in the tank. These ingredients of the sloshing phenomena, that is, liquid natural frequencies and damping, have been the subject of numerous investigations.

Natural frequencies of liquids contained in tanks having a wide variety of shapes and sizes have been determined both analytically and experimentally (refs. 1, 3, and 4). By utilizing this information, sloshing instabilities have been partially averted by designing the guidance and control response frequency away from the lower liquid natural frequencies. Baffle damping has also been the subject of considerable research; references 5, 6, and 7 give information on the relative effectiveness of various types of baffles including annular rings, floating cans, cruciforms, bladders, and conic sections. Some work has also been done on the damping of liquid oscillations in draining tanks containing no baffles (ref. 8). The combined results of these studies define the basic phenomena associated with the sloshing motion. The information derived from these studies is not, however, sufficient in itself to determine the effects of the contained liquid on the dynamic stability of liquid-carrying vehicles. For the examination of stability, the effects of fuel sloshing must be included mathematically in the equations of motion of the vehicle.

The writing of mathematical expressions which describe the liquid motion for inclusion in the vehicle equations of motion presents a difficult problem and has hindered comprehensive stability analyses. The difficulty arises from the complexity of the liquid behavior, the boundary conditions imposed by the vehicle tanks, and the presence of dissipative forces resulting from external damping devices. At the present time, the most promising approach to the problem of including the liquid characteristics in the stability analysis of space vehicles appears to be the simulation of the liquid by means of an analogous mechanical system. Efforts have been devoted to the development of an analog which closely

simulates the hydrodynamic frequencies, forces, and moments. Reference 9 presents an extensive bibliography on fuel-sloshing research which includes a great deal of this work.

One of the more comprehensive treatments of analogous systems is presented in reference 10 which is preceded by the work of references 11, 12, and 13. The hydrodynamic equations for the transverse forces and moments about the base of a partially filled cylindrical tank are presented for planar motions of the cylinder, and a mechanical analog consisting of a fixed mass plus a set of pendulums is then developed which theoretically duplicates the linearized hydrodynamic forces and moments imposed by the undamped liquid on the tank. In the analogous system, the liquid in motion in the region of the free surface is represented by one or more pendulums depending on the number of liquid modes being considered. The remainder of the liquid is assumed to be at rest with respect to the tank and is represented by a fixed mass.

The duplication of the hydrodynamic forces and moments by the analogous system is assured by the proper choice of several physical constants. The values of these constants, expressed in terms of the dimensions of the vehicle, are obtained by a term-by-term comparison of the linearized hydrodynamic equations with the equations of motion of the pendulum analogy.

Several other investigators have suggested analogies which replace the pendulums with spring-mass systems. Probably the most extensive of these works is that of reference 14. To compare the two analogs, reference 15 presents a correlation of the experimental measurement and analytical prediction of the frequencies for free oscillations of a cylindrical tank partially filled with mercury. The liquid is represented analytically by a single pendulum and a fixed mass in one case, and by a spring-mass and fixed-mass combination in the other case. It was concluded in the reported application that the analytical models are identical for small displacements and that they provide excellent simulation of the stiffness and inertial terms for undamped liquid oscillations. The pendulum analogy appears to be the better approach in some applications, such as that of a varying acceleration field, because the pendulum frequencies exhibit the same dependence on the longitudinal accelerations of the tank as do the liquid natural frequencies.

The mechanical analogies thus far discussed have been derived for the case where no external damping is applied to the liquid. The incorporation of damping into these analogies, for use in predicting the dynamic response of systems in which baffles have been installed to provide damping of the liquid, has been limited for two reasons. First, a method for including the damping provided by a baffle is questionable, and secondly, damping values for a given baffle have only recently become available. (See ref. 16.)

Reference 16 presents the results of an experimental program conducted to determine the effects of baffle configuration, size, and location on the damping of the fundamental antisymmetric mode of a liquid oscillating in a static right-circular-cylindrical tank. Emphasis is placed on the damping (in terms of a logarithmic decrement) of the wave amplitude provided by annular ring baffles at various locations with respect to the free surface. Since these data were presented in terms of a logarithmic decrement, an equivalent damping coefficient can

be extrapolated from them which provides a similar decrement for the pendulum motion. Although these damping coefficients apply only to the first antisymmetric liquid mode, it has been shown experimentally (ref. 17) that this mode is of prime importance because of the ease with which large-amplitude liquid motions can be induced and because of the large forces which the liquid pressures impart to the tank wall. It therefore appears that, as a first approximation, the liquid can be treated as a single-degree-of-freedom system and simulated by a single, damped pendulum plus a fixed mass.

It is the purpose of this paper to present the results of a study of the coupled dynamic response of a partially filled cylindrical tank, free to undergo either simultaneous or separate planar pitching and translational oscillations under the influence of a variable self-excitation force. The experimental portion of the investigation was conducted with a laboratory model, while the analytical study was conducted by utilizing an analogous system wherein a damped pendulum is used to simulate the dynamic effects of the liquid. The analytical and experimental results are compared for the purpose of defining the regions of applicability and the limitations of this pendulum analogy for the simulation of the damped liquid.

SYMBOLS

A_1, A_2, A_3	dimensionless parameters defined in equations (A7), (A8), and (A9)
a, b	real and imaginary parts of the complex number $a + ib$
C	arbitrary constants in general equation of motion (eq. (10))
c_α, c_e	viscous damping coefficient, lb-sec/ft
c_γ	viscous damping coefficient, lb-ft-sec/rad
D	damping dissipation function, lb-ft/sec
d	depth of baffle below free surface, ft
F	thrust of engine, lb
f	circular frequency, cps
g	acceleration due to gravity, ft/sec ²
h	distance from tank bottom to quiescent liquid surface, ft
h_1	distance from tank bottom to tank pivot point, ft
I	mass moment of inertia about center of gravity, lb-ft-sec ²

i	imaginary unit = $\sqrt{-1}$
K	spring constant, lb/ft
K_1	tank parameter for fundamental antisymmetric liquid mode = $\xi_1 \frac{h}{r}$
l	length, ft
M	total liquid mass, lb-sec ² /ft
m	mass, lb-sec ² /ft
Q	generalized force
q	generalized coordinate
\bar{q}	initial amplitude of q
r	tank radius, ft
T	kinetic energy, ft-lb
t	time, sec
V	potential energy, ft-lb
ΔW	virtual work, ft-lb
X, Y	Cartesian coordinates
$\alpha, \beta, \gamma, \theta$	angular displacements, radians (See fig. 4.)
Δ	incremental change
δ	logarithmic decrement
λ	root of characteristic equation
ξ_1	first zero of the first derivative of the Bessel function of the first order and first kind
ω	rotational velocity, radians/sec
Subscripts:	
a	any generalized coordinate
c	jet damper
cr	critical damping

cg	center of gravity
e	jet
g	jet pivotal axis
h	pendulum pivot point
k	jet spring
n	number of elements
o	fixed mass
p	pendulum
s	support platform
t	tank
α	coordinate α
β	coordinate β
γ	coordinate γ

A dot over a symbol indicates differentiation with respect to time. For example, $\dot{X} = \frac{dX}{dt}$.

APPARATUS AND INSTRUMENTATION

The apparatus used in the experimental portion of the investigation is shown photographically in figure 1 and is described schematically in figure 2. It consisted of a 12-inch inside-diameter cylindrical tank mounted to be free to translate and pitch in the same plane. An air jet forcing mechanism, free to rotate about an axis normal to the pitch plane, was mounted to the bottom of the cylinder. Additional degrees of freedom were provided by the antisymmetric modes of the liquid contained within the tank. For the purposes of this investigation, only the fundamental antisymmetric liquid mode was considered. Thus the complete system contained four degrees of freedom, namely, tank translation, tank pitching, air jet rotation, and liquid motion. The system was designed so that one or more of these degrees of freedom could be eliminated by the use of simple constraints.

An annular support platform (figs. 1(b) and 2) served as the basic mounting device for the system. The cylindrical tank was concentrically located within this platform and supported by two pivot points attached to the cylinder above the center of gravity of the filled configuration. These pivots constituted the tank pitch axis. The platform was suspended in parallelogram fashion from overhead

supports by means of four wires to allow freedom of tank translation. The translational frequency of the assembled system was governed by the length of the suspension wires and by the stiffness of a spring shown schematically in figure 2. This spring consisted of a rod, placed perpendicular to the plane of system motion, having one end pinned to the support platform and the other end clamped to a rigid wall. Thus, the coupled natural frequencies of the system could be changed simply by replacing a given horizontal rod by another rod having a different stiffness. To obtain a suitable range of coupled frequencies, two different translational springs were employed, one provided coupled frequencies slightly above and the other slightly below the uncoupled liquid natural frequency. Two small support rods, mounted parallel to and in a horizontal plane with the spring rod, constrained the translatory oscillations to the plane of the pitching motions.

The air jet attached to the base of the tank (fig. 1(c)) was used to simulate a gimbaled rocket engine and to provide the desired excitation force. The engine analog was essentially a cylinder having four in-line-nozzle exits along the wall. A shaft integral with and extending outward along the cylinder axis was fitted into bearing supports attached to the base of the propellant tank. Thus, the jet was free to rotate with respect to the tank and in the plane of the tank motion. Air was supplied to the engine through three lightweight vinyl tubes leading from an air storage tank which was maintained at a preselected pressure by control valves at the inlet. A small rod, having a sphere attached to one end, extended downward from the jet shaft into an oil bath. The motion of the sphere through the oil provided external damping of the jet rotation. Therefore, when the tank was given a small displacement, the external damping would cause the thrust vector of the jet to lag this displacement. This lag in turn resulted in destabilizing forces and moments which tended to increase the displacement.

A linear-variable-differential transformer was attached to the support platform to sense the translatory motions of the system. The pitching oscillations were sensed by a strain-gage beam at the pivotal axis of the tank. The output of a selected transducer was amplified and fed into a Dampometer which measured the rate of decay or rate of divergence of the system for various values of liquid damping, thrust, and translatory spring stiffness. Thrust was sensed by a calibrated pressure transducer located in the air jet chamber and connected to a mercury manometer.

Throughout this investigation, water was used as the liquid, and ring baffles with clearance were used to provide the liquid damping. The baffles consisted of 1/8-inch-thick annular Plexiglas rings having a 1/8-inch radial clearance with respect to the tank wall as shown in figure 2. Baffles with 1/2-inch and 3/4-inch widths could be interchanged to vary the amount of damping.

TEST PROCEDURE

In an effort to make a more complete and systematic investigation and to isolate effects of individual parameters, selected subcases were examined before the complete configuration was studied. These subcases are shown schematically in figure 3, and for the purposes of discussion are denoted: two degrees of freedom

(tank translation and liquid motion); three degrees of freedom (tank translation, liquid motion, and jet rotation), with and without thrust; and four degrees of freedom (tank translation, liquid motion, air jet rotation, and tank pitch). Both the experimental and analytical phases of the study were conducted in this order. This study of the successively more complex systems provided a step-by-step evaluation of the effects of various parameters on the system motion. In all tests, the primary variables were the liquid damping, the magnitude of the applied thrust (where applicable), and the system natural frequencies as governed by the spring stiffness.

Basic test procedures were essentially the same for each of the cases examined. In general, the system was manually excited at a frequency closely corresponding to that of a natural mode of oscillation and then released. In all cases, the system amplitude was great enough to permit random responses generated during the excitation to decay before the test data were taken. When a preselected initial liquid amplitude was reached, a signal from the transducer energized the Dampometer which measured damping over a number of cycles of the ensuing oscillation. The frequency was also measured by timing a number of the oscillations with a stop watch. Although the system had two or more natural frequencies in all cases, only those modes were examined in which the system behaved essentially as one having a single degree of freedom upon removal of the excitation. This technique of isolating and examining the characteristics of a single mode was unique for this system and, of course, is not always possible in viewing systems having several degrees of freedom. It was possible in this case only because of the relatively low degree of dynamic coupling between the system elements.

The amount of liquid damping was determined from reference 16 by the size and position of the baffle with respect to the liquid surface and by the liquid amplitude at the time a test point was taken. The thrust level was also preselected by choosing the proper stagnation pressure of air being supplied to the engine. For each test point, constant values of thrust and liquid damping were maintained. The liquid amplitude limits remained fixed for each case under investigation and were of the same order of magnitude as those used in obtaining the damping factors presented in reference 16.

ANALYSIS

Derivation of the Equations of Motion

The mathematical model of the complete system (fig. 2) is shown in figure 4. The liquid is represented by a pendulum and a fixed mass m_0 . The differential equations of motion for this system were developed by use of the Lagrange energy-equation approach (ref. 18). This approach consists of writing the kinetic and potential energies, the damping dissipation function, and the generalized forces in terms of the generalized coordinates of the system. The operations indicated by Lagrange's equations are then performed on the energy expressions. For the present study the generalized coordinates selected were the angular displacements associated with the motions of the tank, liquid (pendulum), and air jet and are designated by α , β , γ , and θ in the mathematical model, figure 4.

The following assumptions are made in the analysis: (1) all angular displacements are small, for example, $\sin \alpha = \alpha$; (2) liquid oscillations are limited to the fundamental antisymmetric liquid mode; and (3) all dissipative forces are the result of viscous damping.

Kinetic energy.- The kinetic energy T of the complete system shown in figure 4 is defined as the summation of the following energy components:
 T_s - kinetic energy of support platform, T_t - kinetic energy of tank,
 T_p - kinetic energy of pendulum, T_o - kinetic energy of fixed mass, and
 T_e - kinetic energy of jet assembly.

The kinetic energy of each of the various elements in terms of the generalized coordinates is as follows:

$$T_s = \frac{1}{2} m_s (\dot{\alpha}_s)^2 \quad (1a)$$

$$T_t = \frac{1}{2} I_{t_{cg}} \dot{\beta}^2 + \frac{1}{2} m_t (\dot{\alpha}_s^2 + 2l_s l_t \ddot{\alpha} \dot{\beta} + l_t^2 \dot{\beta}^2) \quad (1b)$$

$$T_o = \frac{1}{2} I_{o_{cg}} \dot{\beta}^2 + \frac{1}{2} m_o (\dot{\alpha}_s^2 + 2l_s l_o \ddot{\alpha} \dot{\beta} + l_o^2 \dot{\beta}^2) \quad (1c)$$

$$T_p = \frac{1}{2} m_p \left[\dot{\alpha}_s^2 + 2l_s l_h \ddot{\alpha} \dot{\beta} + l_h^2 \dot{\beta}^2 + 2l_p l_h \dot{\beta} (\dot{\gamma} + \dot{\beta}) + 2l_s l_p \ddot{\alpha} (\dot{\gamma} + \dot{\beta}) + l_p^2 (\dot{\gamma} + \dot{\beta})^2 \right] \quad (1d)$$

$$T_e = \frac{1}{2} I_{e_{cg}} (\dot{\beta} + \dot{\theta})^2 + \frac{1}{2} m_e \left[\dot{\alpha}_s^2 + 2l_s l_g \ddot{\alpha} \dot{\beta} + 2l_g l_e \dot{\beta} (\dot{\beta} + \dot{\theta}) + l_g^2 \dot{\beta}^2 + 2l_s l_e \ddot{\alpha} (\dot{\beta} + \dot{\theta}) + l_e^2 (\dot{\beta} + \dot{\theta})^2 \right] \quad (1e)$$

Potential energy.- The total potential energy V of the system consists of the elastic strain energy of the translatory spring and the potential energy of the system resulting from vertical displacements with respect to the equilibrium position. Thus, the total potential energy of the system is:

$$\begin{aligned}
V = & g(m_s + m_t + m_o + m_p + m_e)l_s \frac{\alpha^2}{2} + g(m_t l_t + m_o l_o + m_p l_h + m_e l_g) \frac{\beta^2}{2} \\
& + g m_p l_p \frac{(\beta + \gamma)^2}{2} + g m_e l_e \frac{(\beta + \theta)^2}{2} + \frac{1}{2} K_\alpha (l_s \alpha)^2 \\
& + \frac{1}{2} K_e [l_s \alpha + l_g \beta + l_k (\beta + \theta)]^2
\end{aligned} \tag{2}$$

Dissipation function.- Dissipative forces result from the relative motion between the liquid and the baffles installed to suppress the liquid oscillations. These forces are assumed to be proportional to the relative velocity and are thus treated as dissipative forces resulting from viscous damping. Damping is also present in the translatory spring and the drag mechanism of the air jet. The energy dissipated due to viscous damping is expressed in the form of a dissipation function

$$\begin{aligned}
D = & \frac{1}{2} c_\alpha (l_s \dot{\alpha})^2 + \frac{1}{2} c_\gamma \dot{\gamma}^2 + \frac{1}{2} c_e [l_s^2 \dot{\alpha}^2 + 2l_s l_g \dot{\alpha} \dot{\beta} + 2l_s l_c \dot{\alpha} (\dot{\beta} + \dot{\theta}) + l_g^2 \dot{\beta}^2 \\
& + 2l_g l_c \dot{\beta} (\dot{\beta} + \dot{\theta}) + l_c^2 (\dot{\beta} + \dot{\theta})^2]
\end{aligned} \tag{3}$$

Generalized forces.- The generalized force Q_a associated with each generalized coordinate q_a is defined as

$$Q_a = \frac{\partial(\Delta W)}{\partial(\Delta q_a)} \tag{4}$$

where ΔW is the virtual work, given as the product of the applied force and the virtual displacement Δq_a of the system at the point at which the force is applied. As a result of the thrust F , the virtual work is:

$$\Delta W = -F(\theta + \beta - \alpha)l_s \Delta \alpha - F\theta l_g \Delta \beta \tag{5}$$

Therefore, the generalized forces are

$$Q_\alpha = -Fl_s(\theta + \beta - \alpha) \tag{6}$$

and

$$Q_\beta = -Fl_g \theta \tag{7}$$

Lagrange's equations.— Having derived the system energies, dissipation function, and generalized forces, Lagrange's equations

$$\frac{d}{dt} \left(\frac{\partial T}{\partial \dot{q}_a} \right) - \frac{\partial T}{\partial q_a} + \frac{\partial V}{\partial q_a} + \frac{\partial D}{\partial \dot{q}_a} = Q_a \quad (8)$$

are then used to obtain the differential equations of motion for the system where q_a denotes one of the generalized coordinates α , β , γ , or θ . Then, consistent with the procedures of stability analyses of such systems, the resultant differential equations of motion are assumed to have solutions of the form $q_a = \bar{q}_a e^{\lambda t}$. Upon substituting these assumed solutions into the differential equations of motion, the following matrix results:

$$\begin{bmatrix} \lambda^2 [m_s l_s^2 + m_t l_s^2 + m_o l_s^2 + m_p l_s^2] & \lambda^2 [m_t l_s l_t + m_o l_s l_o + m_p l_s l_h] & \lambda^2 [m_p l_s l_p] & \lambda^2 [m_e l_s l_e] \\ + m_p l_s^2 + m_e l_s^2 & + m_p l_s l_p + m_e l_s l_g + m_e l_s l_e] & & + \lambda [c_e l_s l_c] \\ + \lambda [c_a l_s^2 + c_e l_s^2] & + \lambda [c_e l_s l_g + c_e l_s l_c] & & + 1 [K_e l_s l_k + F l_s] \\ + g [m_s l_s + m_t l_s + m_p l_s + m_o l_s] & + 1 [K_e l_s l_g + K_e l_s l_k + F l_s] & & \\ + m_e l_s + \frac{K_a}{g} l_s^2 + \frac{K_e}{g} l_s^2 - \frac{F}{g} l_s] & & & \\ \lambda^2 [m_t l_s l_t + m_o l_s l_o + m_p l_s l_h] & \lambda^2 [I_t + I_o + I_e + m_t l_t^2 + m_o l_o^2] & \lambda^2 [m_p l_p l_h + m_p l_p^2] & \lambda^2 [I_e + m_e l_g l_e + m_e l_e^2] \\ + m_p l_s l_p + m_e l_s l_g + m_e l_s l_e] & + m_p l_p^2 + 2 m_p l_p l_h + m_p l_h^2 & g [m_p l_p] & + \lambda [c_e l_g l_c + c_e l_c^2] \\ + \lambda [c_e l_s l_g + c_e l_s l_c] & + m_e l_e^2 + 2 m_e l_e l_g + m_e l_g^2] & & + g [m_e l_e + \frac{K_e}{g} l_g l_k] \\ + 1 [K_e l_s l_g + K_e l_s l_k] & + \lambda [c_e l_g^2 + 2 c_e l_g l_c + c_e l_c^2] & & + \frac{K_e}{g} l_k^2 + \frac{F}{g} l_g] \\ + g [m_t l_t + m_o l_o + m_e l_g + m_p l_p] & + g [m_t l_t + m_o l_o + m_e l_g + m_p l_p] & & \\ + m_p l_h + m_e l_e + \frac{K_e}{g} l_k^2 & + m_p l_h + m_e l_e + \frac{K_e}{g} l_k^2 & & \\ + 2 \frac{K_e}{g} l_k l_g + \frac{K_e}{g} l_g^2] & + 2 \frac{K_e}{g} l_k l_g + \frac{K_e}{g} l_g^2] & & \\ \lambda^2 [m_p l_s l_p] & \lambda^2 [m_p l_p l_h + m_p l_p^2] & \lambda^2 [m_p l_p^2] & 0 \\ + g [m_p l_p] & + g [m_p l_p] & + \lambda [c_\gamma] & \\ + g [m_p l_p] & + g [m_p l_p] & + g [m_p l_p] & \\ \lambda^2 [m_e l_s l_e] & \lambda^2 [I_e + m_e l_g l_e + m_e l_e^2] & 0 & \lambda^2 [I_e + m_e l_e^2] \\ + \lambda [c_e l_g l_c] & + \lambda [c_e l_g l_c + c_e l_c^2] & & + \lambda [c_e l_c^2] \\ + 1 [K_e l_s l_k] & + g [m_e l_e + \frac{K_e}{g} l_g l_k] & & + g [m_e l_e + \frac{K_e}{g} l_k^2] \\ + \frac{K_e}{g} l_k^2] & + \frac{K_e}{g} l_k^2] & & \end{bmatrix} \begin{Bmatrix} \alpha \\ \beta \\ \gamma \\ \theta \end{Bmatrix} = \begin{Bmatrix} 0 \\ 0 \\ 0 \\ 0 \end{Bmatrix} \quad (9)$$

It should be noted that the equations of motion of the system under consideration are homogeneous since the generalized forces are functions only of the generalized coordinates and thus appear on the left side of the matrix.

Solutions of the Equations of Motion

The system of homogeneous equations will have a nontrivial solution if and only if the determinant of the characteristic matrix vanishes. An expansion of this determinant will yield an eighth order polynomial in terms of λ , the solution of which yields the characteristic roots to define the stability of the coupled system. The determination of the numerical values of the coefficients in the determinant is presented in the appendix.

The expansion of the determinant and the solution of the resultant polynomial were accomplished by the use of an IBM 704 electronic data processing machine. In all cases, the roots were in the form of complex conjugate pairs $\lambda_n = a_n \pm ib_n$, where the number of pairs n was of course equal to the number of degrees of freedom being considered. The resultant stability of the coupled system is readily apparent from an examination of these roots. If the real parts of all of the complex pairs are negative, the system is stable; however, if one or more of the real parts is positive, an unstable condition is indicated.

The equation of motion for each generalized coordinate has a final form,

$$q_a = C_1 e^{\lambda_1 t} + C_2 e^{\lambda_2 t} + \dots + C_n e^{\lambda_n t} \quad (10)$$

Although all of the roots are included in this equation, in many cases one root becomes predominant after a short period of time. For the cases considered in this investigation, for example, one or more of the roots usually had relatively large negative real parts. Thus, after a short period of time, these roots had a negligible effect on the resultant motion. In such a case the system will oscillate in essentially a pure mode at a frequency given by the imaginary part b of the remaining characteristic root. The logarithmic decrement of the resultant motion is given by $\delta = \frac{-2\pi a}{b}$.

PRESENTATION AND DISCUSSION OF RESULTS

General

In order to examine the applicability of the pendulum analogy for the simulation of the liquid characteristics under conditions similar to those encountered by an actual space vehicle, a model having four degrees of freedom was experimentally and analytically examined. The primary degrees of freedom were the planar translatory and pitching motions of the cylindrical tank and the oscillation of the contained liquid. The rotation of the air jet about its axis constituted the

fourth degree of freedom. Since the mass of this element was relatively small, the addition of the air jet, exclusive of thrust, had an almost negligible effect on the dynamic response of the system. It did, however, provide a source of excitation for the purpose of examining the degree of simulation afforded by the analogy under divergent conditions. Variables affecting the stability of the system and thus considered in this study were the liquid damping coefficient c_γ , the thrust F , and the coupled natural frequencies as governed by the horizontal spring constant K_α .

It is reiterated that in all cases the differential equations of motion of the system yielded two or more pairs of roots λ and consequently, two or more coupled natural frequencies f depending on the number of degrees of freedom included in the analysis. The analysis, however, did not yield the resultant equations of motion which depend on the initial conditions of the excitation. Therefore in checking the theoretical results and thus the applicability of the analogy, an attempt was made to compare the theoretical roots, that is, the damping and coupled frequencies of the dominant modes with those obtained experimentally.

Although the degree of applicability of the analogy has been based on the experimental examination of one mode in some cases, this technique is believed to be justified since the dominant mode examined appeared to be the only mode that could lead to an unstable condition and thus a possible failure of a space-flight system.

Two-Degree-of-Freedom System

The results obtained for the two-degree-of-freedom system involving motion of the contained liquid and tank translation are shown in figure 5. In this figure the damping of the modes, in terms of the logarithmic decrement, are presented for a range of liquid-damping coefficients c_γ .

Figure 5(a) presents the results for the system employing the smaller translational spring having an elastic constant of 106 lb/ft. Theoretical decrements are shown for both modes, but experimental data are presented only for the first mode. In this case, the fundamental mode consisting primarily of tank translation completely dominated the oscillation regardless of the initial excitation as a result of its relatively low damping. The data points presented for the fundamental mode represent an average of five or more measured values for a given test condition. The figure shows that the theoretical response is in good agreement with the experimental results and that the damping of the fundamental mode is directly proportional to the liquid damping coefficient. The modal damping at $c_\gamma = 0$ is due to the structural damping c_α . It should be noted that this structural damping has a more pronounced effect on the first mode where the ratio of tank translational amplitude to liquid amplitude is higher than that for the second mode. Also presented in the figure are the average experimental and theoretical frequencies. For the fundamental mode, the theoretical frequency (1.09 cps) is in close agreement with the average experimental value (1.11 cps). For the

range covered in this study, no significant changes in frequency occurred as the liquid damping coefficient c_γ was varied.

Figure 5(b) shows the damping of the two modes for the system equipped with the larger spring having an elastic constant of 340 lb/ft. In this case the decrements of both modes were of the same relative magnitude and both could therefore be examined. Again the logarithmic decrements in question appear to vary directly with the liquid damping coefficients c_γ and are in excellent agreement with the experimental values. For this particular case, the structural damping of the system was found to have a negligible effect. Therefore, the damping of the modes approaches zero as the damping coefficient c_γ approaches zero. The theoretical frequencies of the modes were 1.53 and 2.24 cps which are in excellent agreement with the experimental results of 1.53 and 2.22 cps.

In examining figures 5(a) and (b), it is interesting to compare the magnitudes of the modal damping. Those modes having frequencies nearest that of the uncoupled liquid natural frequency (1.73 cps) are the most highly damped. This result appears somewhat contradictory since this condition has been cited as the most critical fuel-sloshing situation. For the particular configuration under examination however, the decay rate depends upon the relative magnitudes of the total system energy and the dissipative energy. The dissipative energy is almost entirely due to the liquid motion - the amplitude range of which remained constant for all studies. When the system coupled frequency is near that of the liquid natural frequency, smaller inputs (tank translational amplitudes) are required to generate the initial liquid amplitude and thus the total system energy level is relatively low. The high ratio of liquid amplitude to tank displacement, although a potential source of a sloshing instability, results in a higher ratio of dissipative energy to total system energy and thus a greater decay rate in the case of a free vibration.

Three-Degree-of-Freedom System Without Thrust

The free vibration characteristics of the three-degree-of-freedom system involving tank translation, liquid motion, and air jet rotation, are shown in figure 6. These results are very similar to those obtained for the two-degree-of-freedom case. The addition of the relatively low mass of the air jet system had a very small effect on the frequencies of the dominant modes. The jet did increase the damping of the modes for a given value of c_γ as a result of the added damping present in the system. The additional mode resulting from the action of the air jet could not be detected experimentally. According to the theory, this mode has extremely high damping and was therefore not included in the figure.

For the range examined, the decrements of the modes again appear to be directly proportional to the coefficient of liquid damping c_γ . The agreement between the theoretical and experimental results illustrates the excellent simulation of the liquid behavior afforded by the pendulum analogy.

Three-Degree-of-Freedom System With Thrust

To examine the ability of the pendulum analogy to simulate the dynamic characteristics of the liquid under conditions approaching instability, the self-excited system (fig. 3(b)) was employed. The characteristics of the dominant modes were examined throughout a range of thrust levels for two values of the liquid damping coefficient c_γ . The results of this phase of the investigation are shown in figure 7. The logarithmic decrement of the fundamental mode of the system incorporating the smaller spring is shown as a function of thrust level in figures 7(a) and 7(b). Figure 7(a) shows the effects of thrust for a high value of the damping coefficient $c_\gamma = 0.0214$, while figure 7(b) presents the results obtained by using a lower value of the damping coefficient $c_\gamma = 0.00729$. The figure indicates the destabilizing effect of the thrust on the decay of the fundamental mode, that is, as the thrust level increases the decay rate of the mode decreases and finally becomes unstable or diverges. For the case of the higher liquid damping coefficient, a higher thrust level is tolerable before an unstable condition is encountered. In comparing the theoretical and experimental results, the theoretical value of damping indicated for a given thrust level appears to be somewhat higher than that obtained experimentally. In view of the excellent correlation in the free vibration cases however, this discrepancy may be attributed to changes in the characteristics of the engine apparatus with the addition of thrust. If, for example, the engine damping coefficient c_e increased slightly with the addition of thrust, the engine would have a proportionally higher destabilizing effect. Very slight variations in the engine damping coefficient were found theoretically to produce variations in the results of the order of magnitude shown in figures 7(a) and 7(b).

The results obtained for the system having the larger translational spring constant are presented in figures 7(c) and 7(d). The damping factors for both of the modes are shown at various thrust levels for two values of c_γ . Both modes have essentially the same damping factor at $F = 0$ for each case but exhibit a marked dissimilarity as F is increased above zero. In both figures, 7(c) and 7(d), the theory predicts that the damping of the higher mode, involving primarily tank translation, will not be greatly affected by the thrust level. This prediction is substantiated by the agreement obtained between the experimental and the analytical results. The theory further predicts that the lower mode damping will be inversely proportional to the applied thrust, that is, higher thrust values will yield lower values of system damping. No experimental results are presented to document this predicted trend because of a difficulty encountered in isolating this mode. While subjected to thrust, the system was observed to beat thus yielding very erratic experimental damping values. The absence of the beating phenomenon in the higher mode is due to the relatively high translational amplitude required to attain the initial liquid amplitude. In the lower mode however, the translational amplitude was sufficiently low to permit the occurrence of beating between the translational oscillation and the liquid oscillation.

A better understanding of the modal behavior may be gained by considering the relative phase relationships existing between the moving liquid and the tank during oscillation in each of the modes. When the system was excited such that the higher mode was predominant, the liquid motion was out of phase with the tank

displacement since the frequency of the excitation was above that of liquid resonance. Thus, the liquid exerts a more pronounced stabilizing influence on the system by opposing the destabilizing force. Conversely, lower mode excitation resulted in liquid oscillations which were in phase with the tank displacement and resulted in a destabilizing influence on the system. From these observations, the dissimilarity of the damping-thrust curves for the two modes is not surprising.

Four-Degree-of-Freedom System

The theoretical damping-thrust relationships for the fundamental mode of the complete four-degree-of-freedom system, involving tank translation, tank pitch, liquid motion, and air jet rotation, are presented in figure 8(a) for three values of c_γ . The fundamental mode in this case is predominantly a pitching oscillation. Again the theory predicts a destabilizing effect with either increasing thrust or decreasing liquid damping, however no correlation of these results could be obtained experimentally. Since the theoretical frequency (0.83) was found to be in good agreement with that obtained experimentally (0.82), the poor damping-thrust correlation suggested that the damping coefficients assumed for a given baffle location (ref. 16) might not be applicable for a system undergoing pitching oscillations.

In an effort to examine more closely the applicability of the assumed damping coefficients c_γ for a pitching system, the results of figure 8(a) were replotted in figure 8(b) to show the theoretical thrust at neutral stability ($\delta = 0$) as a function of c_γ . Consistent with previous observations, the results show a linear increase in thrust at neutral stability with an increase in c_γ . In an effort to check this prediction experimentally, the thrust level at neutral stability was measured for several different baffle positions. The values of c_γ were obtained from reference 16 for the size and location of the baffle. For convenience, the applicable results of reference 16 are presented in figure 9 where the damping coefficient c_γ is shown as a function of baffle position d/r for the particular baffles employed in this investigation. These reference data show a decrease in c_γ as the baffle is further submerged below $\frac{d}{r} \approx 0.06$. If these damping coefficients, obtained from the decay of the liquid amplitude in a static tank, are applicable for a pitching system, the experimental thrust at neutral stability will decrease as the baffle is submerged as shown by the theoretical curve in figure 8(c) since the theory of figure 8(b) predicts a linear variation of this thrust with c_γ . However, this prediction was not borne out experimentally. In fact, the thrust level for neutral stability was observed to increase in some cases as the baffle was further submerged. These experimental results are also shown in figure 8(c) where the thrust for neutral stability is shown as a function of baffle location.

In comparing theory and experiment, it appears that in a pitching tank, the damping at a given baffle location differs from that indicated in figure 9. It must be noted that the data of figure 9 however were obtained from the decay of the fundamental antisymmetric liquid mode in a static tank. Although these data have been assumed to be applicable for both translational and pitching tanks, it

appears that a baffle in a pitching tank is effective throughout a much greater depth range than the same baffle in a static or translating tank.

The existence of a greater effective range of a baffle in a pitching tank was later documented by the data presented in figure 10 wherein the decrement of the fundamental pitching mode is presented as a function of baffle location d/r . For both the 1/2-inch and 3/4-inch ring baffles with clearance, the data show that the damping factor associated with the fundamental pitching mode reaches a maximum at $\frac{d}{r} \approx 1$, and then slowly decreases as the baffle is further submerged. The slight peak noted in the data at $\frac{d}{r} \approx 0.3$ is most probably due to a combination of the translatory damping and the pitch damping. At values of $\frac{d}{r} \geq 0.4$, the translational damping becomes negligible and the remainder of the curve may be considered as representing only the liquid pitch damping. The effective depth range of the same baffles installed in a static tank is restricted to values of $\frac{d}{r} \leq 0.6$.

The increased effectiveness of the baffle in suppressing pitching oscillations is understandable after examining the behavior of the liquid with respect to the tank. When the liquid oscillations are confined to a static tank or to a tank in pure translation, the liquid at depths greater than one radius is essentially at rest with respect to the tank. Thus a baffle installed in the region $\frac{d}{r} \geq 0.6$ has a negligible effect on the damping since there is no relative motion between the liquid and the baffle. The situation changes radically when the motion of the tank is predominantly one of pitching. Small tufts of yarn placed along the tank wall in the pitch plane revealed that the tank essentially rotates about the liquid mass or that there is relative motion between the entire liquid mass and the tank. Consequently a baffle installed in a pitching tank remains effective at much greater depths than does a baffle in a static or translating tank. It should be noted that the data of figure 10 serve only as an illustration of the damping trends or baffle effectiveness in a pitching tank. The damping factor shown for the fundamental mode is unique for the particular location of the pivotal axis.

In view of the limited studies of the pitching characteristics of the system, the discrepancies noted in the four degree-of-freedom system are easily explained. The most obvious discrepancy appears to be the effective liquid damping coefficient associated with the pitching. In particular, the damping associated with a given baffle in a fixed tank, as published in reference 16, while applicable for a translating tank, is not applicable in the case of a pitching tank. It appears that for consistent results, damping terms associated with both the translational mode and the pitching mode must be included in the analysis. At the present time, there is no literature relating to the damping provided by a baffle in a pitching tank. Therefore pending an investigation of the damping of liquids in pitching tanks with baffles, the applicability of the pendulum analogy in predicting the modal damping of such a system is questionable.

Frequency Comparison

The modal frequencies of free vibration for all of the configurations are summarized in table I. The configurations are classified according to degrees of freedom and translational spring constant. The theoretical modal frequencies are presented in the order of their numerical occurrence and are compared with the measured experimental frequencies. It should be noted that the mode resulting from the addition of the air jet could not be excited experimentally and therefore no experimental data are presented.

The correlation between the theory and the experiment indicates the excellent simulation of the stiffness and inertia of the liquid afforded by the pendulum analogy. The results further indicate that the addition of a pitching degree of freedom does not limit the applicability of the analogy for frequency studies. In considering the cases examined, it appears that the analogy can be used for frequency studies in any system that experiences planar oscillations.

CONCLUDING REMARKS

An analytical and experimental investigation has been conducted to determine the coupled dynamic response of a tank partially filled with liquid and undergoing free and forced planar oscillations. The results of this investigation are as follows:

1. For the range of baffle damping considered in this investigation, an increase in the liquid damping resulted in a marked increase in the damping of the predominant modes of the system.
2. The more highly damped mode for the system having only coupled tank translation and liquid motion was that mode having a frequency nearest the uncoupled natural frequency of the liquid. This mode involved primarily liquid motion, thus the ratio of dissipative energy to total-system energy was relatively high and resulted in proportionally higher modal damping.
3. The pendulum analogy affords an excellent simulation of the liquid for the analytical prediction of the coupled natural frequencies of a liquid-tank combination undergoing planar oscillations.
4. In cases wherein the tank motion is purely translatory, the pendulum analogy may be used in predicting the modal damping, and thus the dynamic response of the system, if the pendulum is damped such that its decrement is equal to the decrement of liquid amplitudes in an identical static tank fitted with the same baffle configuration.
5. Although useful in predicting the coupled natural frequencies, the pendulum analogy, incorporating damping values found applicable in the translating tank, does not yield valid modal damping for the same configuration undergoing pitching oscillations. This discrepancy is apparently due to a basic difference

found to exist between the damping of a liquid in a translating tank and of a liquid in the same tank undergoing pitching oscillations.

6. The difference in damping characteristics of a liquid in a translating tank and the liquid in the same tank undergoing planar pitching oscillations is the direct result of a dissimilarity in the relative motion existing between the liquid and tank in each system. In a translating tank relative motion exists between the liquid and tank wall primarily in the region of the liquid surface, while in a pitching tank, relative motion takes place at all points of liquid-tank contact. Consequently, a baffle in a pitching tank has a greater effective depth range and thus entirely different damping characteristics.

Langley Research Center,
National Aeronautics and Space Administration,
Langley Station, Hampton, Va., May 28, 1963.

APPENDIX

DETERMINATION OF PHYSICAL PARAMETERS OF SYSTEM

The numerical values for the physical parameters involved in the equations of motion are presented in table II and were obtained as follows: The characteristics of the pendulum analogy were calculated using the results of reference 10; and, the remainder of the parameters were either directly or indirectly obtained from physical measurements.

With respect to the pendulum analogy, the following quantities (see fig. 4) were calculated: m_p - mass of the pendulum, l_p - length of the pendulum, l_h - distance from tank pivotal axis to pendulum pivot, m_o - the fixed mass, l_o - distance from tank pivotal axis to center of gravity of fixed mass, and I_o - mass moment of inertia of fixed mass. It was found (ref. 10) that the analogous system would exactly duplicate the hydrodynamic forces and moments if:

$$m_p = M(A_1) \quad (A1)$$

$$l_p = g/\omega^2 \quad (A2)$$

$$l_h = h_1 - (hA_2/A_1) \quad (A3)$$

$$m_o = M(1 - A_1) \quad (A4)$$

$$l_o = h_1 - \left[h \left(\frac{1}{2} + \frac{r^2}{4h^2} - A_2 \right) / (1 - A_1) \right] \quad (A5)$$

$$I_o = Mh^2 \left(\frac{1}{3} + A_3 - A_2 \right) - M(h_1 - l_o)^2 \quad (A6)$$

where the dimensionless parameters A_1, A_2, A_3 are defined for the fundamental antisymmetric mode of the liquid oscillation as:

$$A_1 = \frac{2 \tanh K_1}{K_1 (\xi_1^2 - 1)} \quad (A7)$$

$$A_2 = 2 \frac{1}{K_1^2} \frac{2 + K_1 \sinh K_1 - \cosh K_1}{(\xi_1^2 - 1) \cosh K_1} \quad (A8)$$

$$A_3 = \frac{1}{K_1^3} \frac{2 \sinh K_1 - K_1}{(\xi_1^2 - 1) \cosh K_1} \quad (A9)$$

and

$$K_1 = \xi_1 \frac{h}{r} \quad (A10)$$

where

ξ_1 first zero of the first derivative of the Bessel function of the first order and first kind (that is, $J_1'(\xi) = 0$ at $\xi = \xi_1 = 1.84$)

M total mass of the liquid

h liquid depth

r tank radius

h_1 distance from the tank bottom to the tank pitch axis

The natural frequency of the fundamental antisymmetric mode ω is then,

$$\omega = \sqrt{\frac{g \xi_1}{r} \tanh \frac{\xi_1 h}{r}} \quad (A11)$$

The coefficient of damping c_γ was obtained from the damping results of reference 16 where the logarithmic decrement of the fundamental antisymmetric mode is presented as a function of baffle location d/r , where d is the distance from the quiescent liquid surface to the baffle. For each of the baffle locations used in this investigation, the damping coefficient was obtained from figure 5 of reference 16 by equating the given decrement to

$$\delta = 2\pi \frac{c_\gamma}{c_{\gamma cr}} \frac{1}{\sqrt{1 - \left(\frac{c_\gamma}{c_{\gamma cr}}\right)^2}} \quad (A12)$$

where $c_{\gamma cr}$ is the critical damping coefficient of the pendulum.

The remaining numerical coefficients were evaluated as follows: m_s - mass of support platform, m_t - mass of tank, and m_e - mass of engine were measured directly prior to assembling the system; l_s - length of support wires, l_g - distance from tank pivotal axis to pivotal axis of jet, and l_c - distance from jet pivotal axis to jet damper were also measured directly; l_t - distance from the

pivotal axis of tank to center of mass of the empty tank, and l_e - distance from jet pivotal axis to center of mass of the jet assembly were obtained by balancing the elements in question on knife-edge supports, to determine the locations of their respective centers of mass.

The mass moments of inertia of the tank and engine assembly, I_t and I_e were obtained indirectly by measuring the natural frequency of the individual elements when oscillated about their respective pivotal locations. The spring constants of the cantilever rods K_α employed in this investigation were obtained from measurements of the translatory natural frequencies of the empty tank configuration. The structural damping coefficient associated with the spring c_α and the damping coefficient of the engine assembly c_e were obtained by measuring the logarithmic decrement of the individual systems and equating the decrements:

$$\left. \begin{aligned} \delta_\gamma &= 2\pi \frac{c_\gamma}{c_{\gamma cr} \sqrt{1 - \left(\frac{c_\gamma}{c_{\gamma cr}}\right)^2}} \\ \delta_e &= 2\pi \frac{c_e}{c_{e cr} \sqrt{1 - \left(\frac{c_e}{c_{e cr}}\right)^2}} \end{aligned} \right\} \quad (A13)$$

and

The thrust of the air jet F was obtained from a calibration of engine thrust in pounds as a function of the internal pressure of the jet tank. This calibration was obtained by mounting the engine on a balance scale and obtaining the required air pressure for a given thrust level. Finally, the gravitational constant g was taken as 32.16 ft/sec².

REFERENCES

1. McCarty, John Locke, and Stephens, David G.: Investigation of the Natural Frequencies of Fluids in Spherical and Cylindrical Tanks. NASA TN D-252, 1960.
2. Bauer, Helmut F.: Propellant Sloshing. Rep. No. DA-TR-18-58 (C AB 71091), Dev. Operations Div., Army Ballistic Missile Agency (Redstone Arsenal, Ala.), Nov. 5, 1958.
3. McCarty, John Locke, Leonard, H. Wayne, and Walton, William C., Jr.: Experimental Investigation of the Natural Frequencies of Liquids in Toroidal Tanks. NASA TN D-531, 1960.
4. Leonard, H. Wayne, and Walton, William C., Jr.: An Investigation of the Natural Frequencies and Mode Shapes of Liquids in Oblate Spheroidal Tanks. NASA TN D-904, 1961.
5. Miles, J. W.: Ring Damping of Free Surface Oscillations in a Circular Tank. Jour. Appl. Mech., vol. 25, no. 2, June 1958, pp. 274-276.
6. Abramson, H. Norman, and Ransleben, Guido E., Jr.: A Note on the Effectiveness of Two Types of Slosh Suppression Devices. Tech. Rep. No. 6 (Contract No. DA-23-072-ORD-1251), Southwest Res. Inst., June 15, 1959.
7. Stofan, Andrew J., and Pavli, Albert J.: Experimental Damping of Liquid Oscillations in a Spherical Tank by Positive-Expulsion Bags and Diaphragms. NASA TN D-1311, 1962.
8. Stephens, David G., Leonard, H. Wayne, and Perry, Tom W., Jr.: Investigation of the Damping of Liquids in Right-Circular Cylindrical Tanks, Including the Effects of a Time-Variant Liquid Depth. NASA TN D-1367, 1962.
9. Cooper, R. M.: Dynamics of Liquids in Moving Containers. ARS Jour., vol. 30, no. 8, Aug. 1960, pp. 725-729.
10. Schmitt, Alfred F.: Forced Oscillations of a Fluid in a Cylindrical Tank Oscillating in a Carried Acceleration Field - A Correction. Rep. ZU-7-074 (Contract No. AF04(645)-4), CONVAIR - Astronautics, Feb. 4, 1957.
11. Kachigan, K.: Forced Oscillations of a Fluid in a Cylindrical Tank. Rep. ZU-7-046 (Contract No. AF04(645)-4), CONVAIR, Oct. 4, 1955.
12. Graham, E. W.: The Forces Produced by Fuel Oscillation in a Rectangular Tank. Rep. No. SM-13748, Douglas Aircraft Co., Inc., Apr. 13, 1950.
13. Lorell, Jack: Forces Produced by Fuel Oscillations. Progress Rep. No. 20-149 (Contract No. DA-04-495-Ord 18), C.I.T. Jet Propulsion Lab., Oct. 16, 1951.

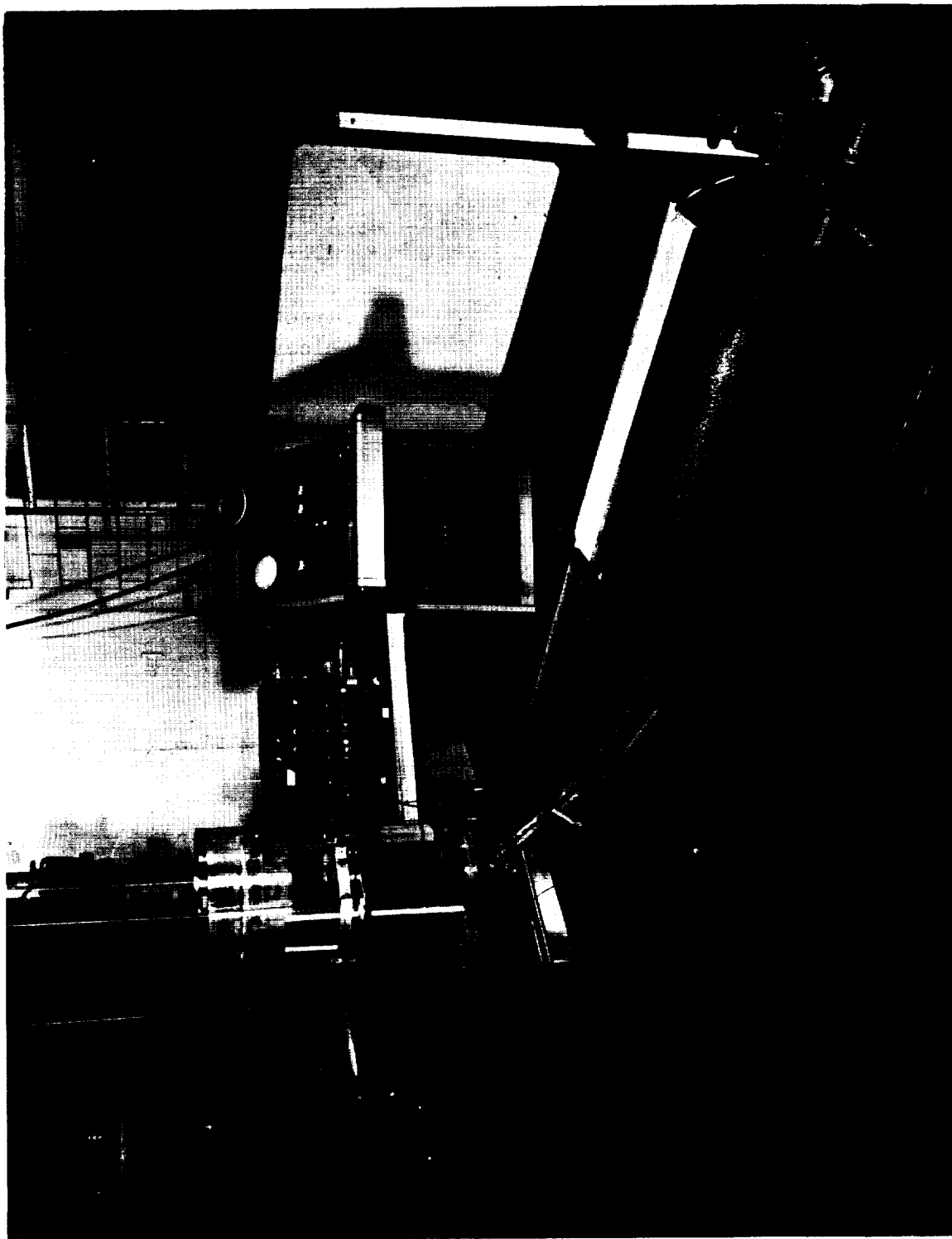
14. Bauer, Helmut F.: Theory of the Fluid Oscillations in a Circular Cylindrical Ring Tank Partially Filled With Liquid. NASA TN D-557, 1960.
15. Warner, Robert W., and Caldwell, John T.: Experimental Evaluation of Analytical Models for the Inertias and Natural Frequencies of Fuel Sloshing in Circular Cylindrical Tanks. NASA TN D-856, 1961.
16. Silveira, Milton A., Stephens, David G., and Leonard, H. Wayne: An Experimental Investigation of the Damping of Liquid Oscillations in Cylindrical Tanks With Various Baffles. NASA TN D-715, 1961.
17. Eulitz, Werner: The Sloshing Phenomenon and the Mechanism of a Liquid in Motion in an Oscillating Missile Container. Rep. Nr. DS-R-31, Dev. Operations Div., Army Ballistic Missile Agency (Huntsville, Ala.), Oct. 1957.
18. Timoshenko, Stephen: Vibration Problems in Engineering. Second ed., D. Van Nostrand Co., Inc., 1937, pp. 189-222.

TABLE I.- EXPERIMENTAL-THEORETICAL FREQUENCY COMPARISON

Degrees of freedom	Translational spring constant, K_a , lb/ft	Experimental frequency, cps	Theoretical frequency, cps
Two	106	1.11 1.92	1.09 1.94
	340	1.53 2.22	1.53 2.24
Three	106	1.11 ----- 1.91	1.08 1.49 1.93
	340	----- 1.53 2.21	1.49 1.55 2.22
Four	340	0.82 ----- 1.55 2.60	0.83 1.38 1.53 2.61

TABLE II.- NUMERICAL VALUES OF PHYSICAL PARAMETERS

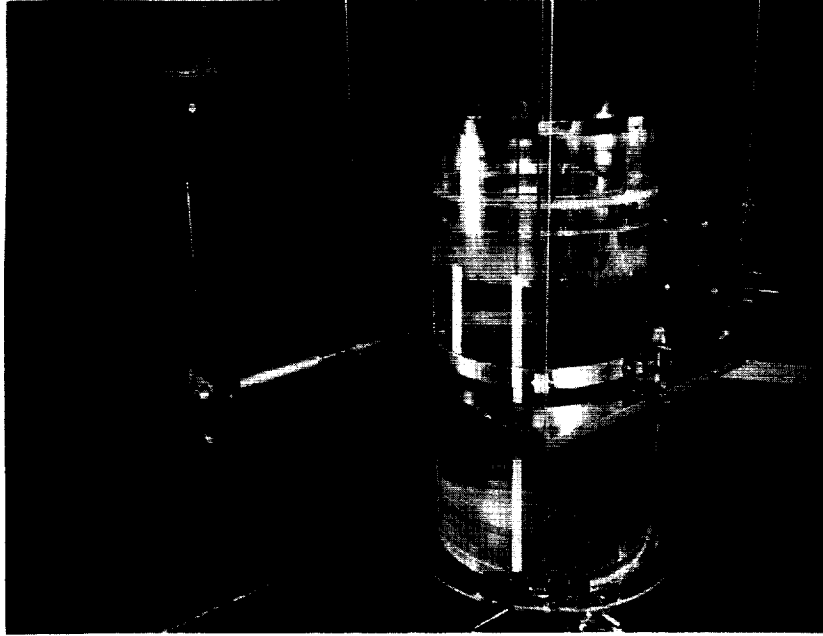
Parameter	Symbol	Numerical value	Method of determination
Length	l_c	0.63 ft	Direct measurement
	l_e	.07 ft	Direct measurement
	l_g	1.16 ft	Direct measurement
	l_h	-.23 ft	Calculated (ref. 10)
	l_k	-----	Not used
	l_o	.20 ft	Calculated (ref. 10)
	l_p	.27 ft	Calculated (ref. 10)
	l_s	4.79 ft	Direct measurement
	l_t	.32 ft	Direct measurement
Mass	m_e	0.062 lb-sec ² /ft	Direct measurement
	m_o	1.674 lb-sec ² /ft	Calculated (ref. 10)
	m_p	.340 lb-sec ² /ft	Calculated (ref. 10)
	m_s	.123 lb-sec ² /ft	Direct measurement
	m_t	.540 lb-sec ² /ft	Direct measurement
Inertia	I_e	0.00122 lb-ft-sec ²	From rotational frequency
	I_o	.117 lb-ft-sec ²	Calculated (ref. 10)
	I_t	.258 lb-ft-sec ²	From rotational frequency
Spring constant	K_e	-----	Not used
	K_a	106.0 and 340.0 lb/ft	From translatory frequency
Damping coefficient	c_e	0.00917 lb-sec/ft	From measured decrement
	c_a	.0848 lb-sec/ft	From measured decrement
	c_γ	Variable (ft-lb-sec/radian)	From reference 16
Force	F	Variable (lb)	Calibration of jet
Acceleration	g	32.16 ft/sec ²	Sea-level standard



L-62-2049

(a) General view.

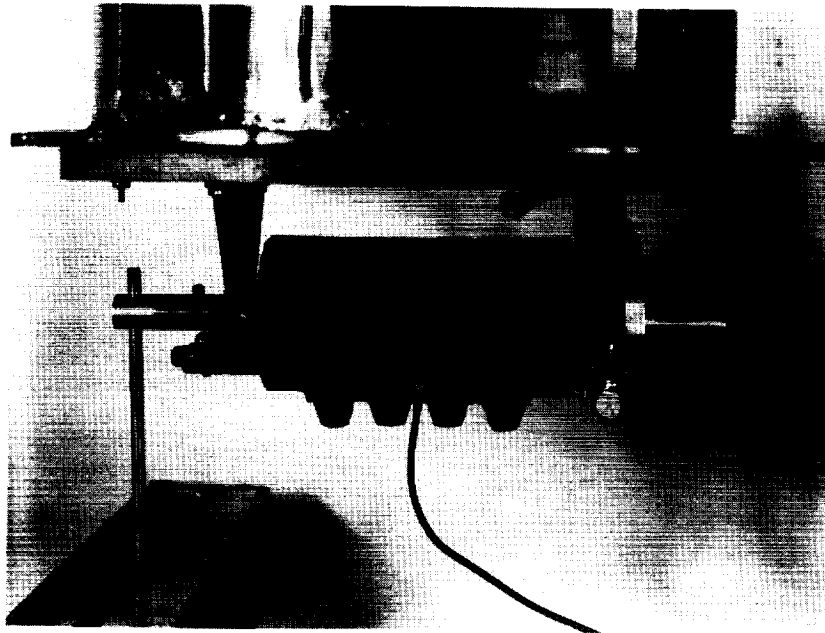
Figure 1.- Apparatus and instrumentation.



(b) Tank and mounting assembly.

L-62-2045

Figure 1.- Continued.



(c) Air jet assembly.

L-62-2046

Figure 1.- Concluded.

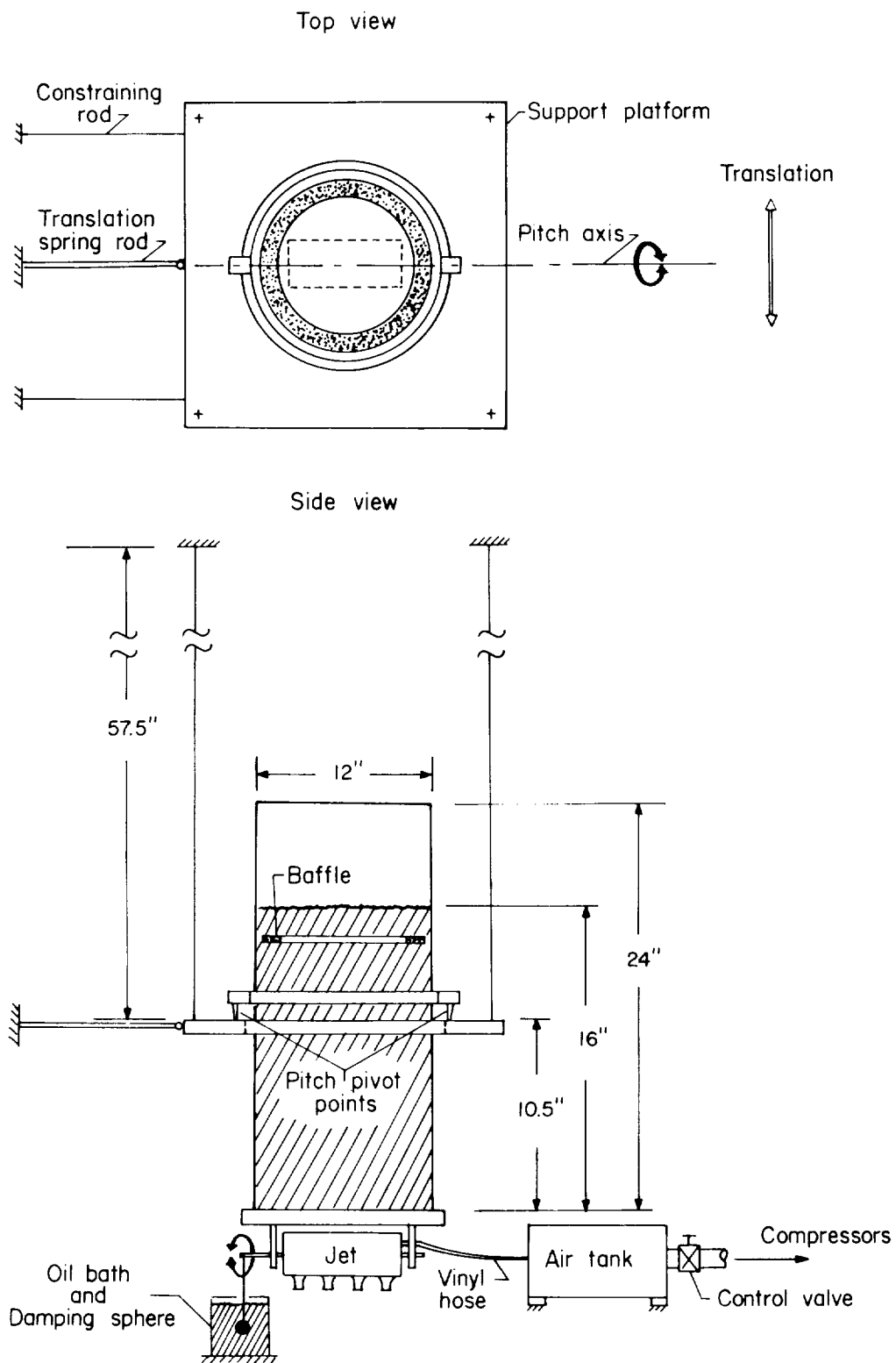
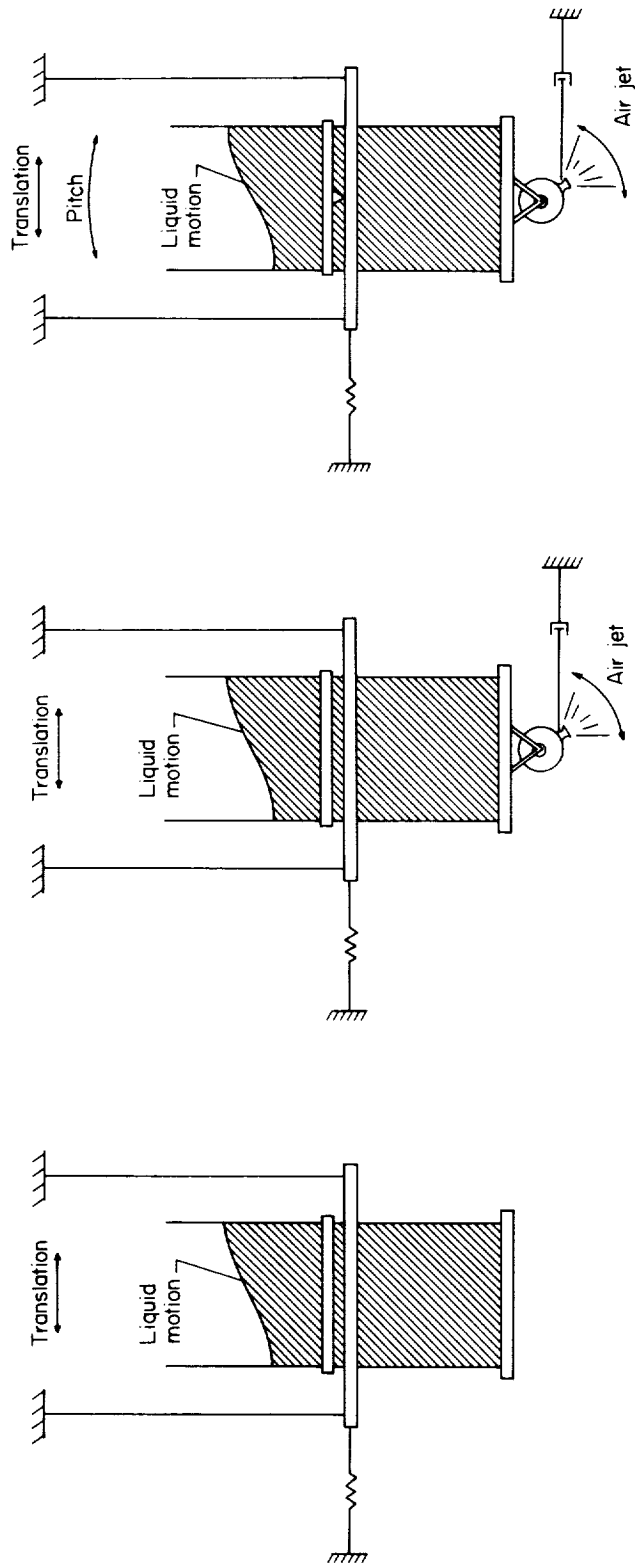


Figure 2.- Schematic of experimental apparatus.

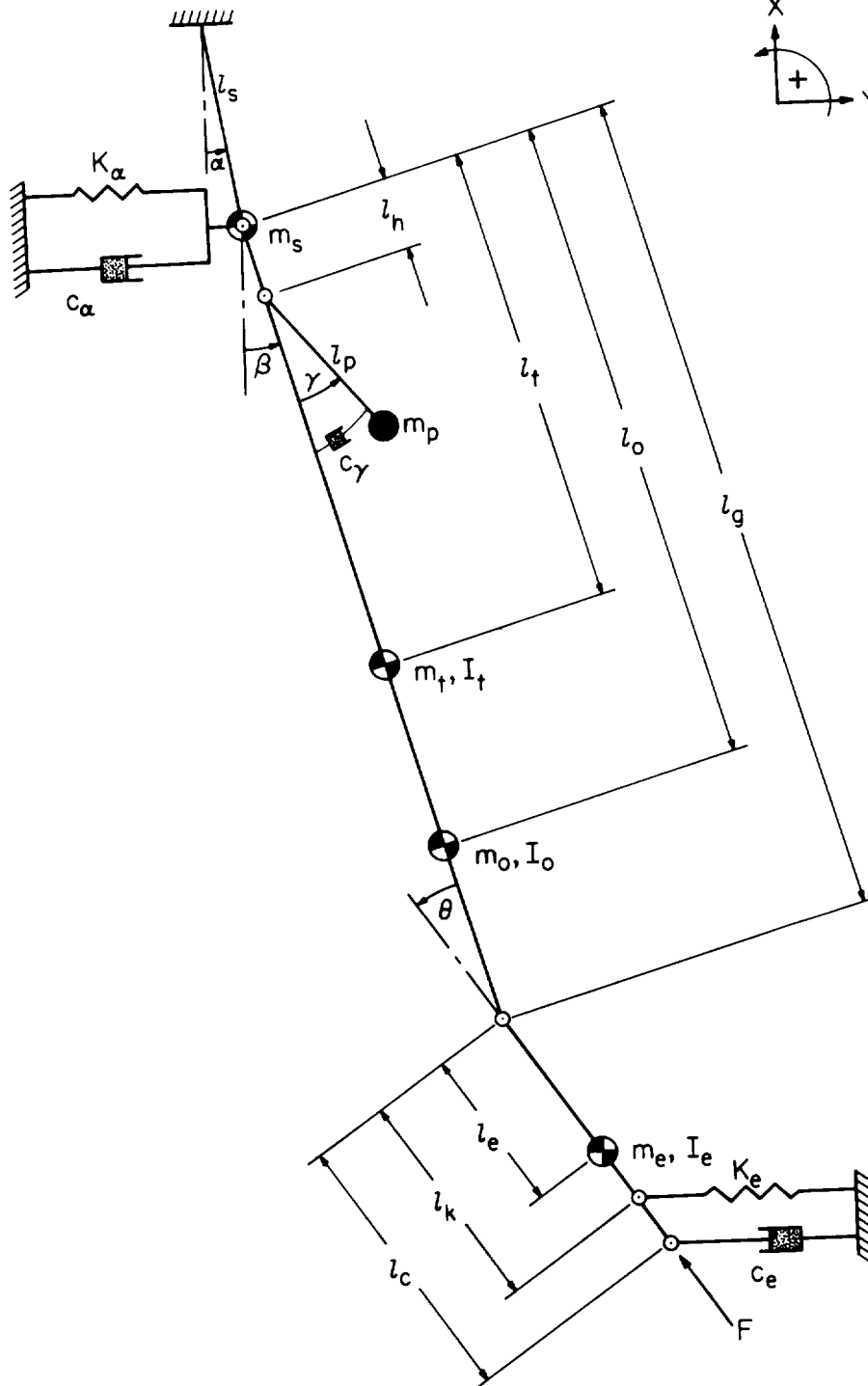


(a) Two degrees of freedom (liquid motion, tank translation).

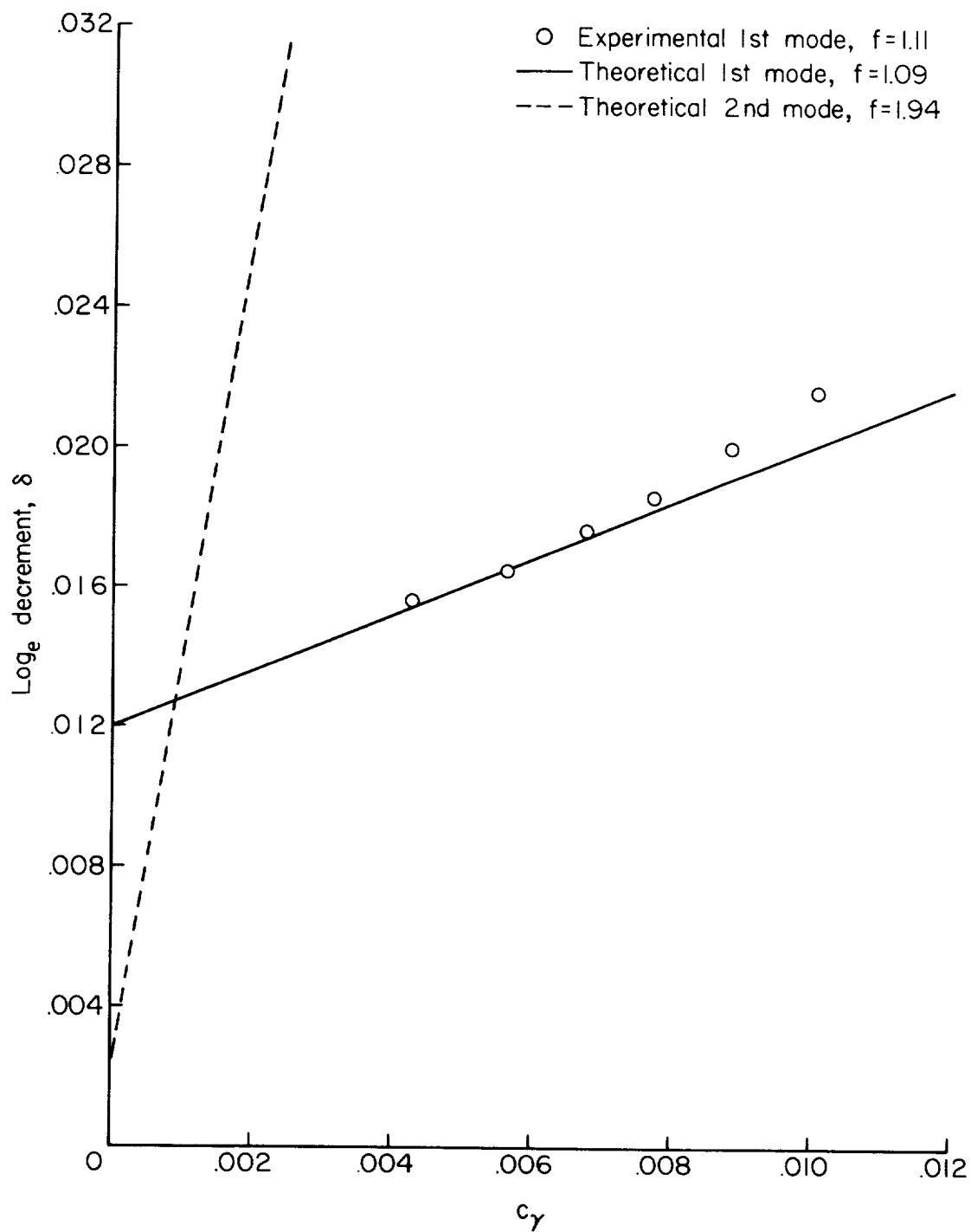
(b) Three degrees of freedom (liquid motion, tank translation, air jet rotation).

(c) Four degrees of freedom (liquid motion, tank translation, air jet motion, tank pitch).

Figure 3.- Schematic representation of cases investigated.

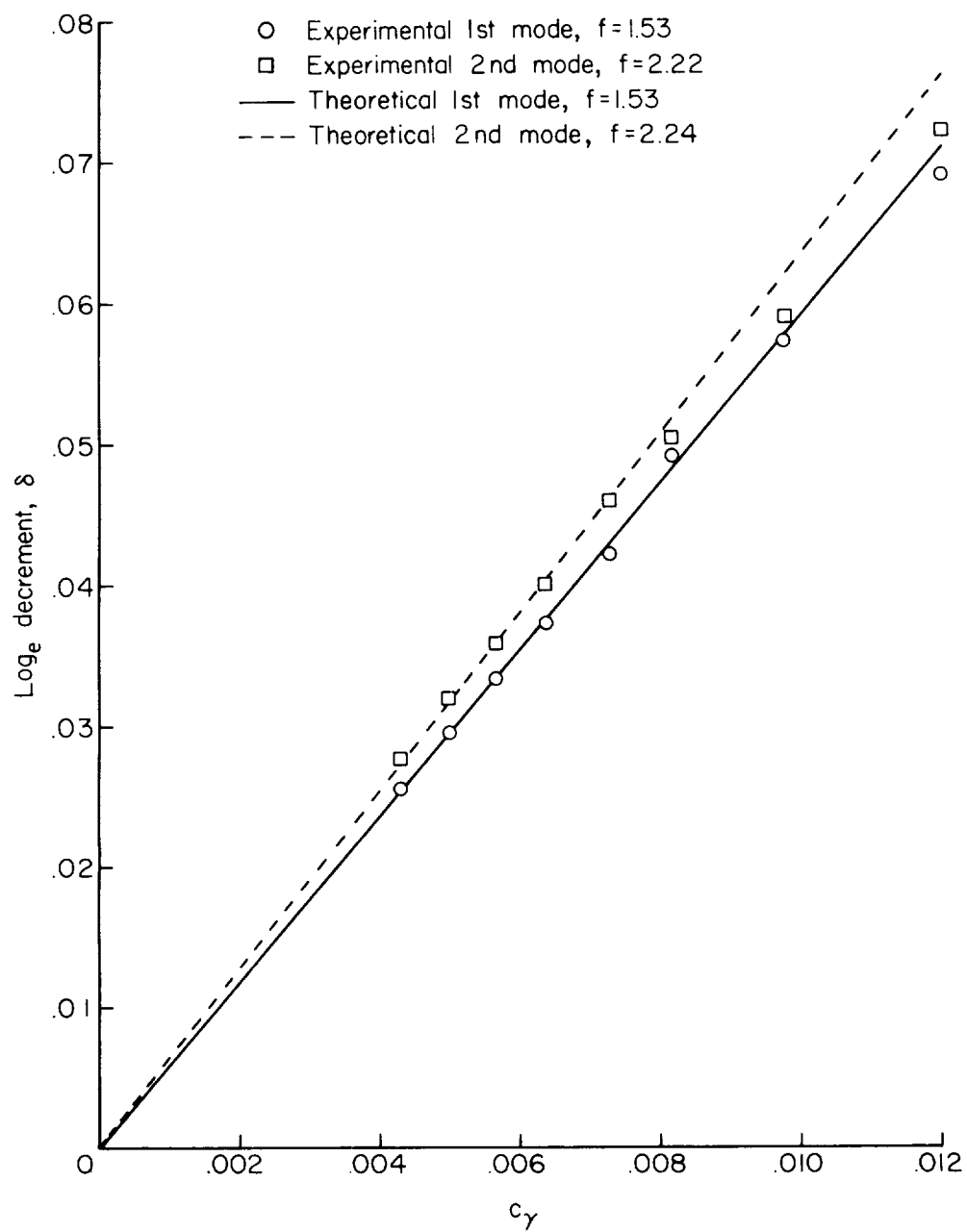


31



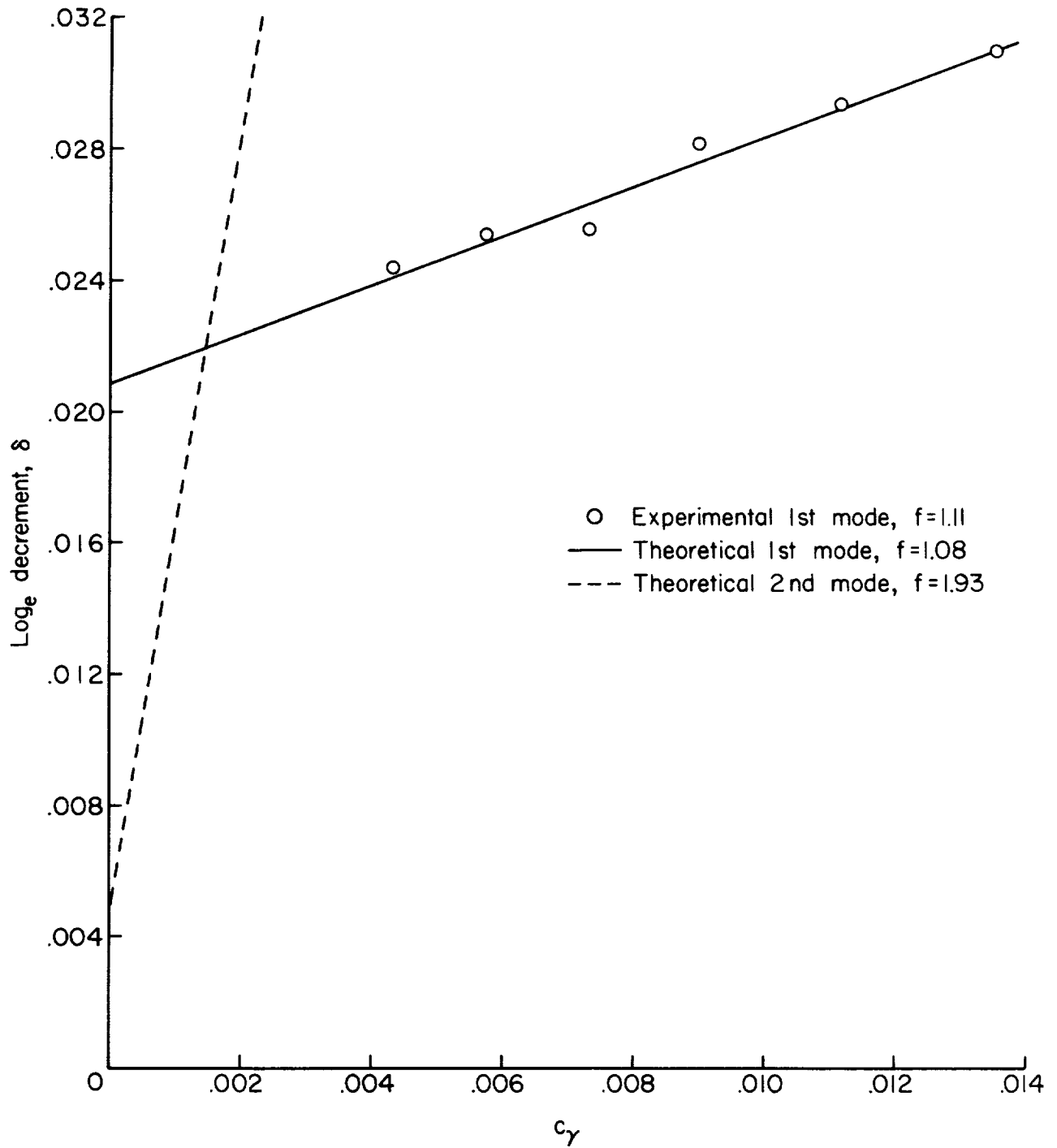
(a) $K_a = 106$.

Figure 5.- Variation of modal damping with liquid damping coefficient for two degree-of-freedom system (tank translation, liquid motion).



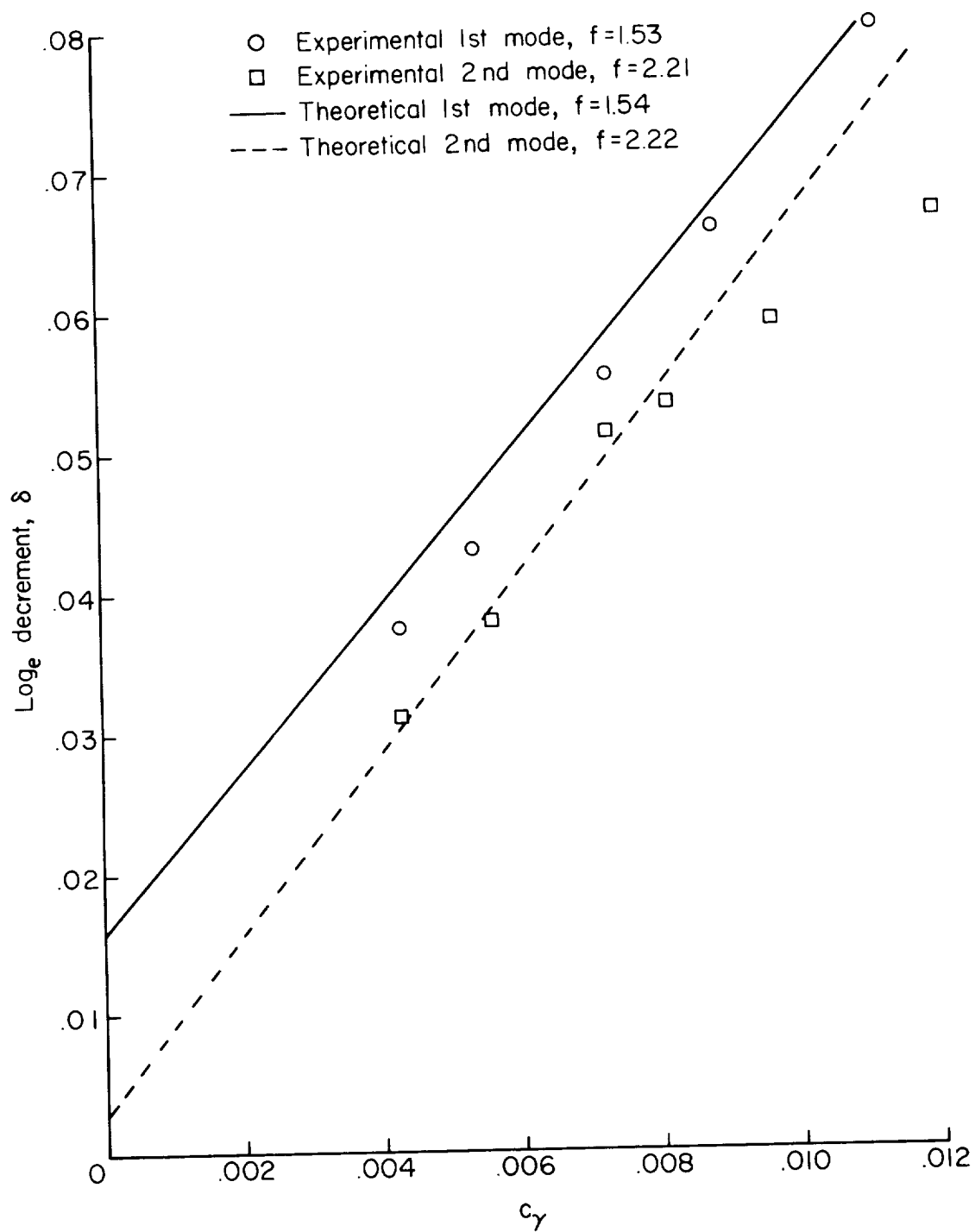
(b) $K_a = 340$.

Figure 5.- Concluded.



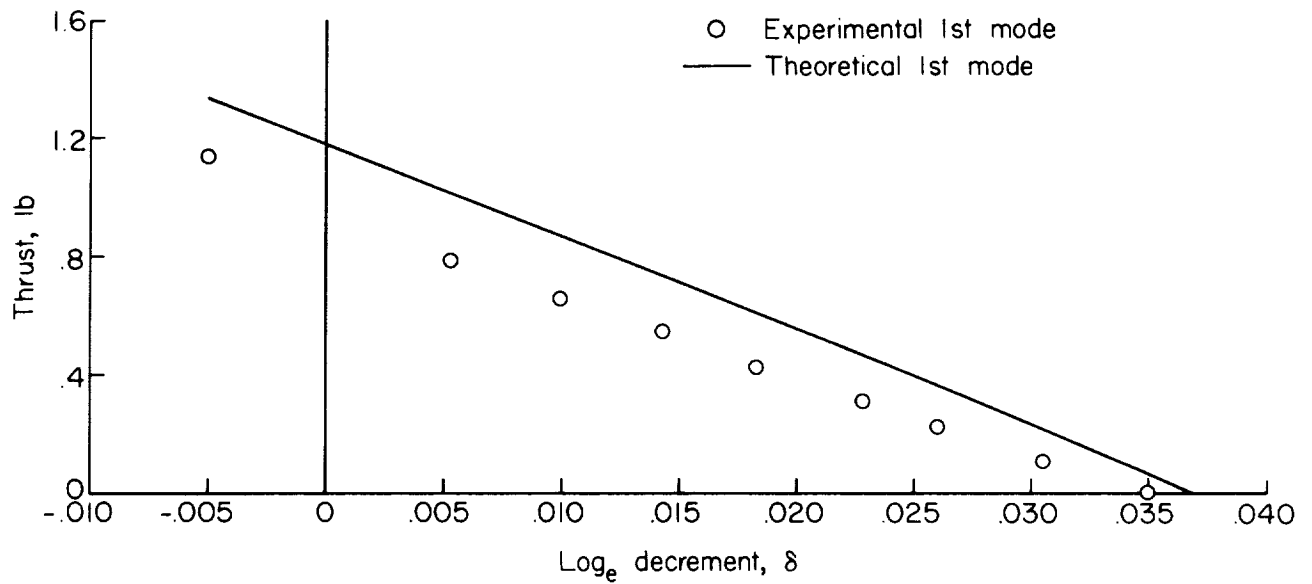
(a) $K_a = 106$; $F = 0$.

Figure 6.- Variation of modal damping with liquid damping coefficient for three degree-of-freedom system (tank translation, liquid motion, air jet rotation).

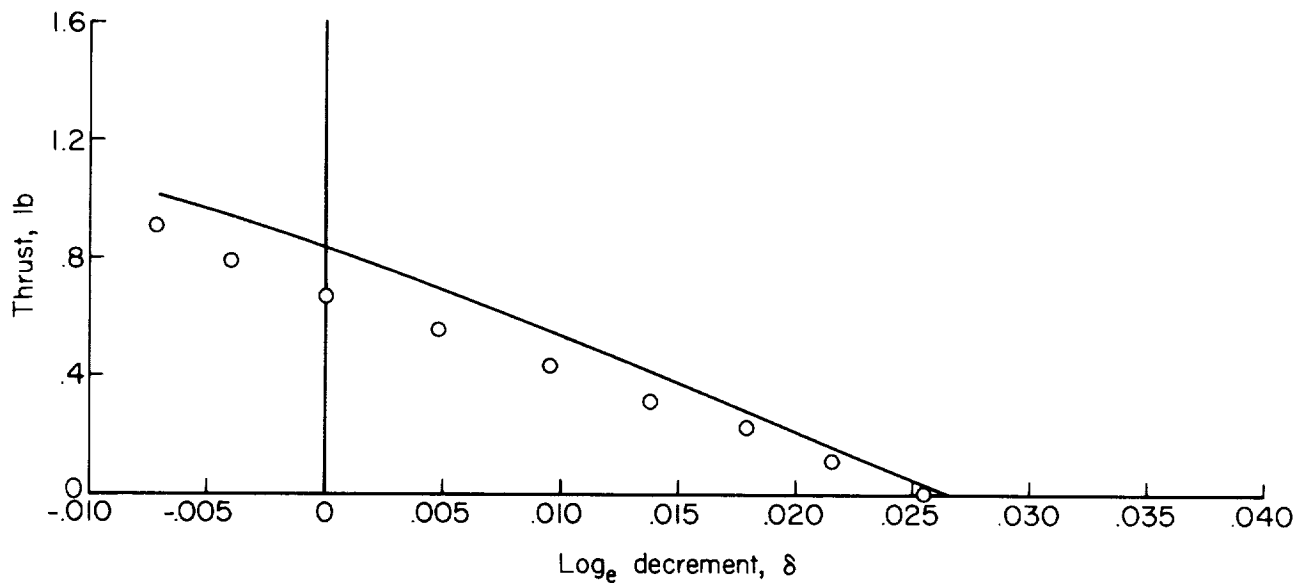


(b) $K_\alpha = 340$; $F = 0$.

Figure 6.- Concluded.

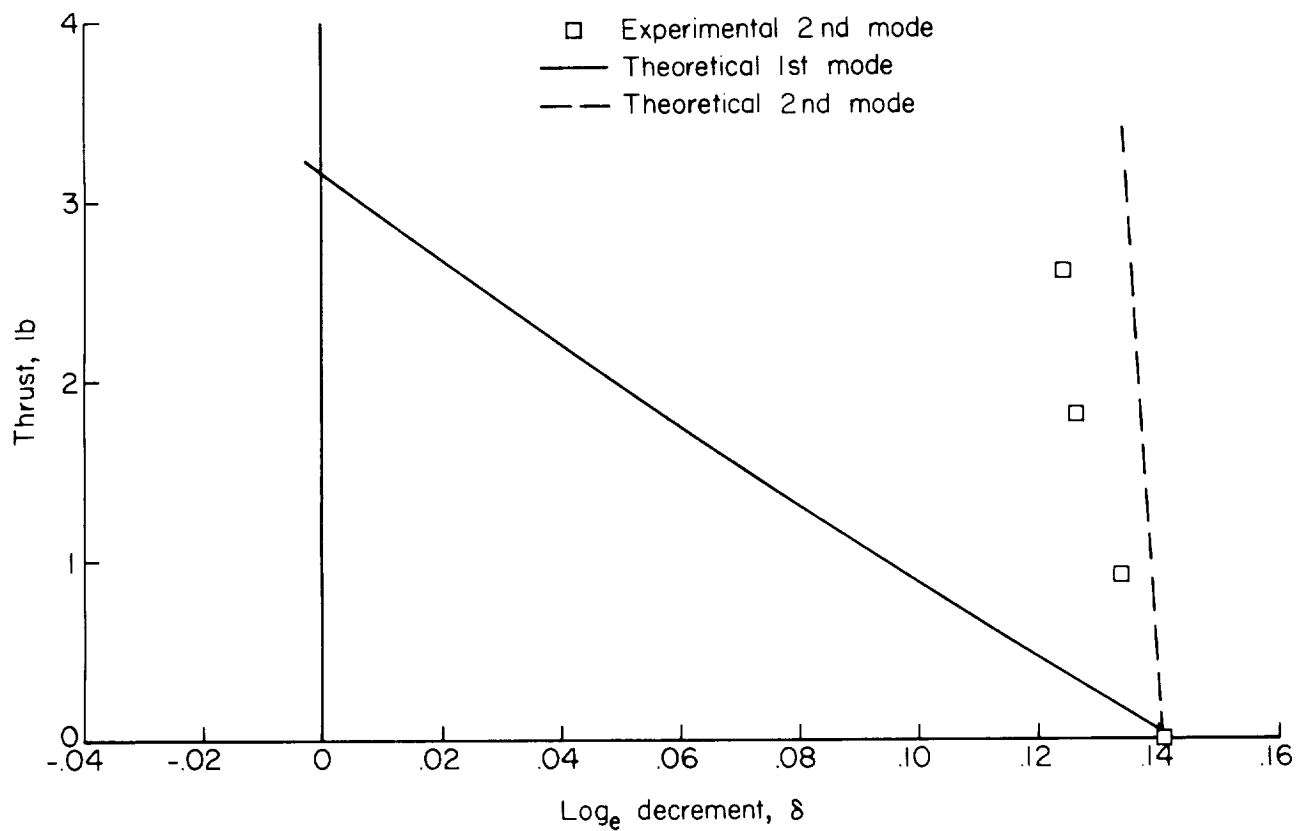


(a) $c_\gamma = 0.0214$; $K_\alpha = 106$.

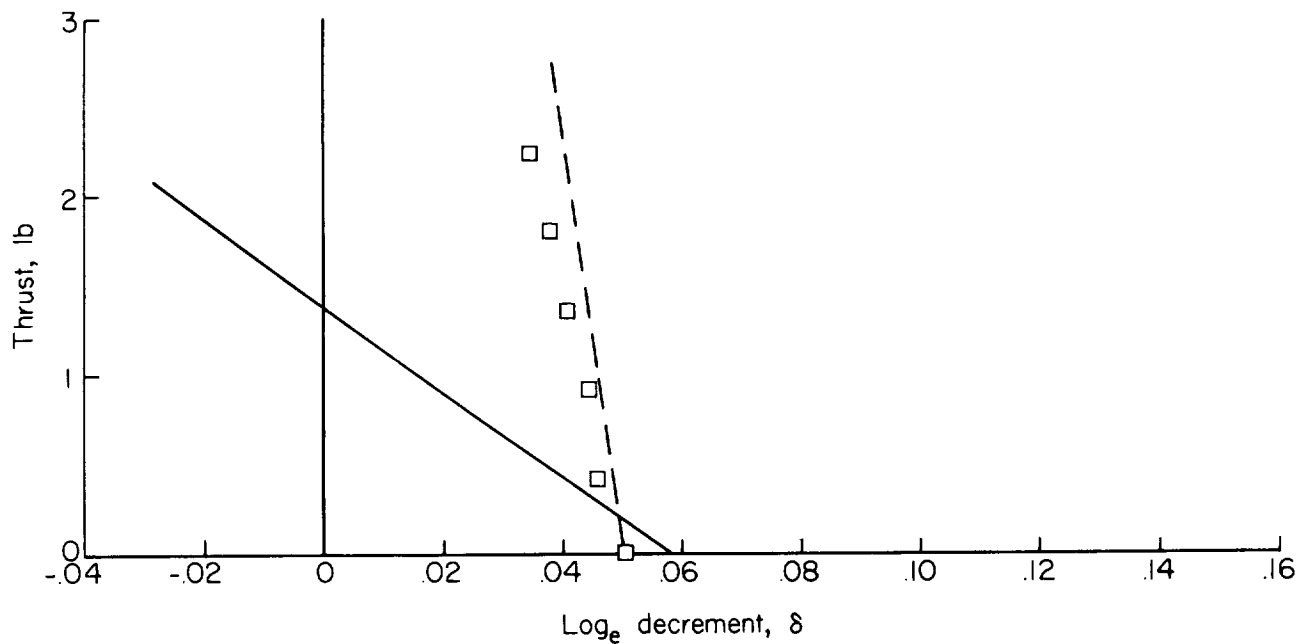


(b) $c_\gamma = 0.00729$; $K_\alpha = 106$.

Figure 7.- Variation of modal damping with thrust level. Three-degree-of-freedom system.

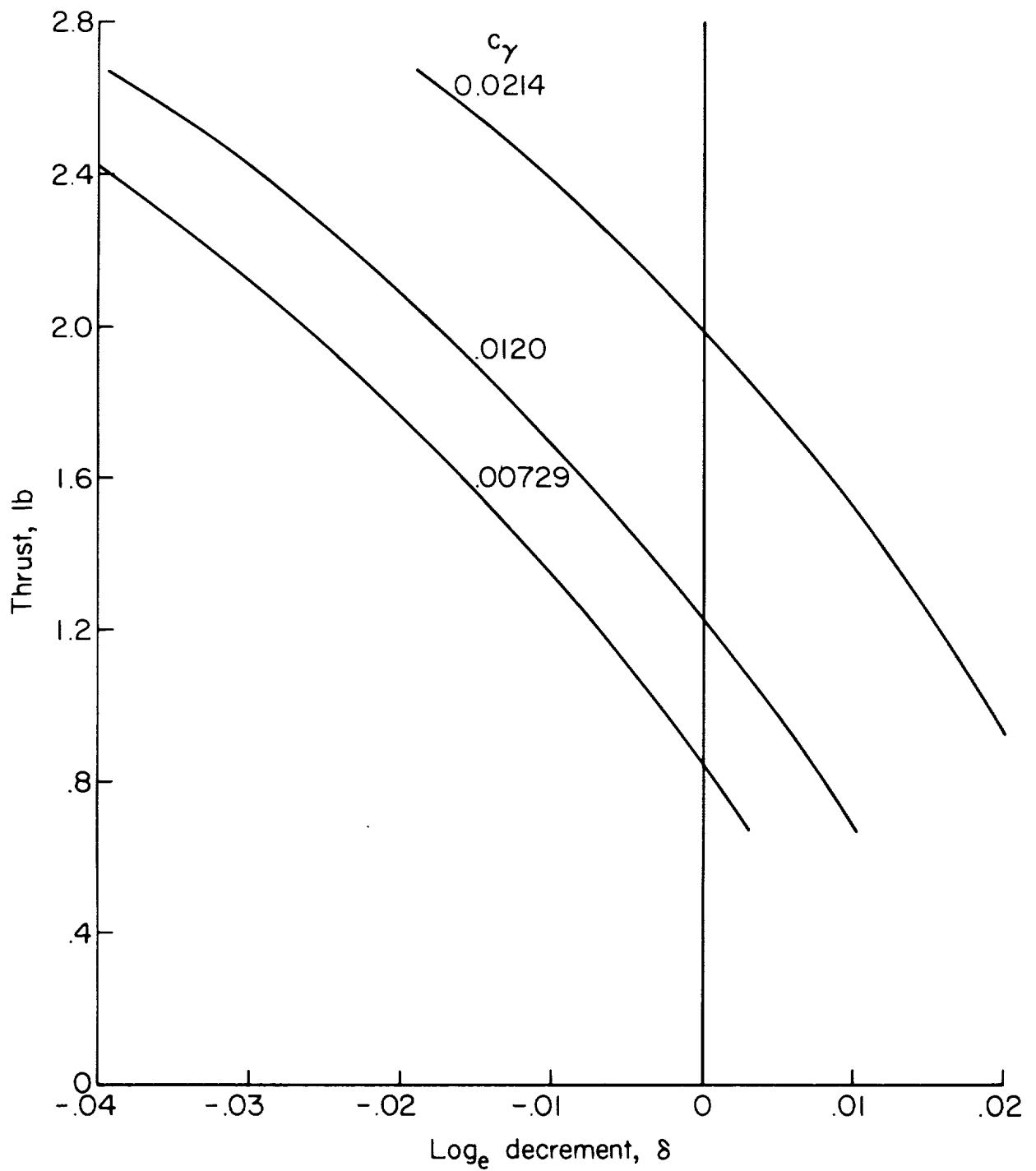


(c) $c_\gamma = 0.0214$; $K_\alpha = 340$.



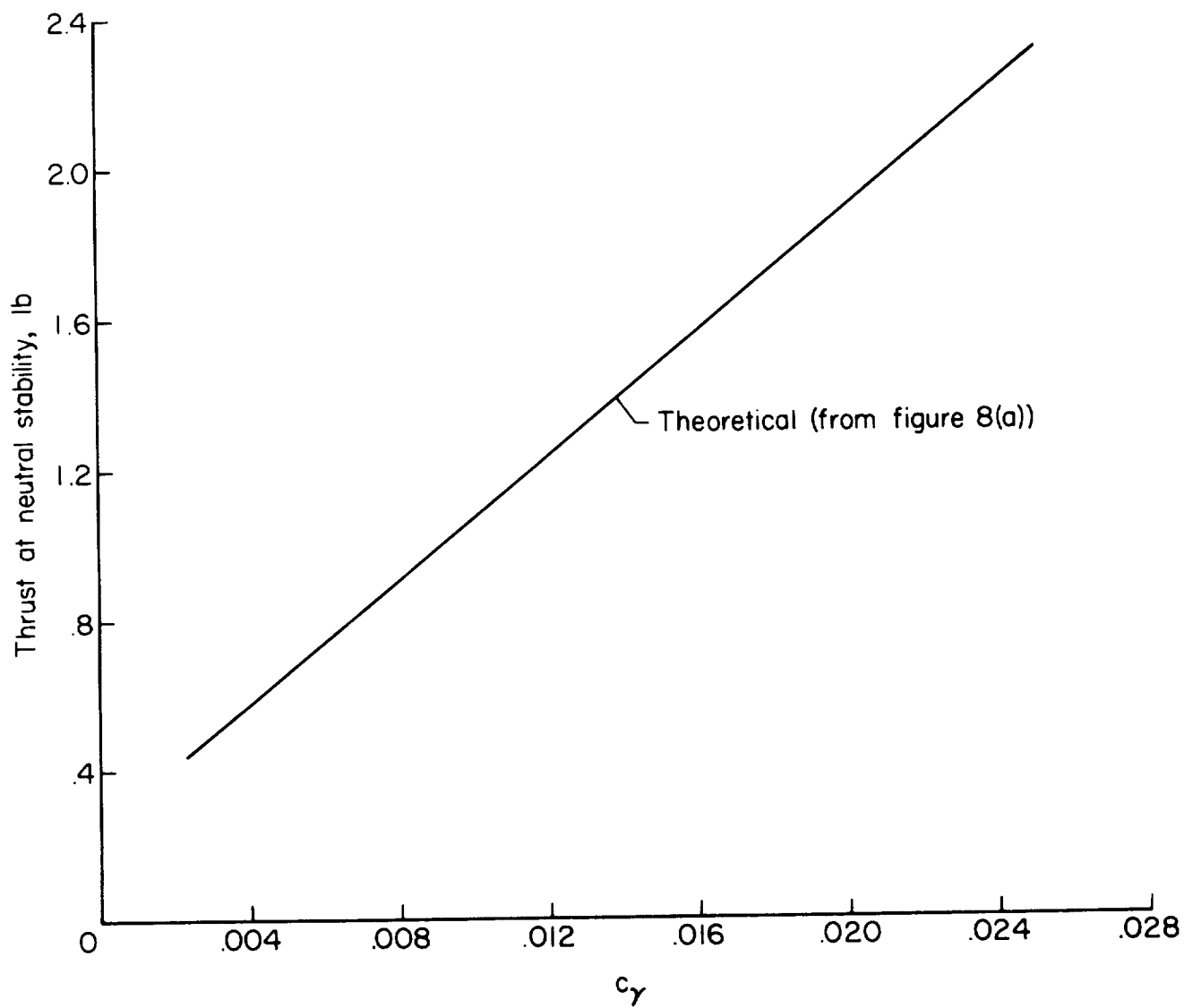
(d) $c_\gamma = 0.00729$; $K_\alpha = 340$.

Figure 7.- Concluded.



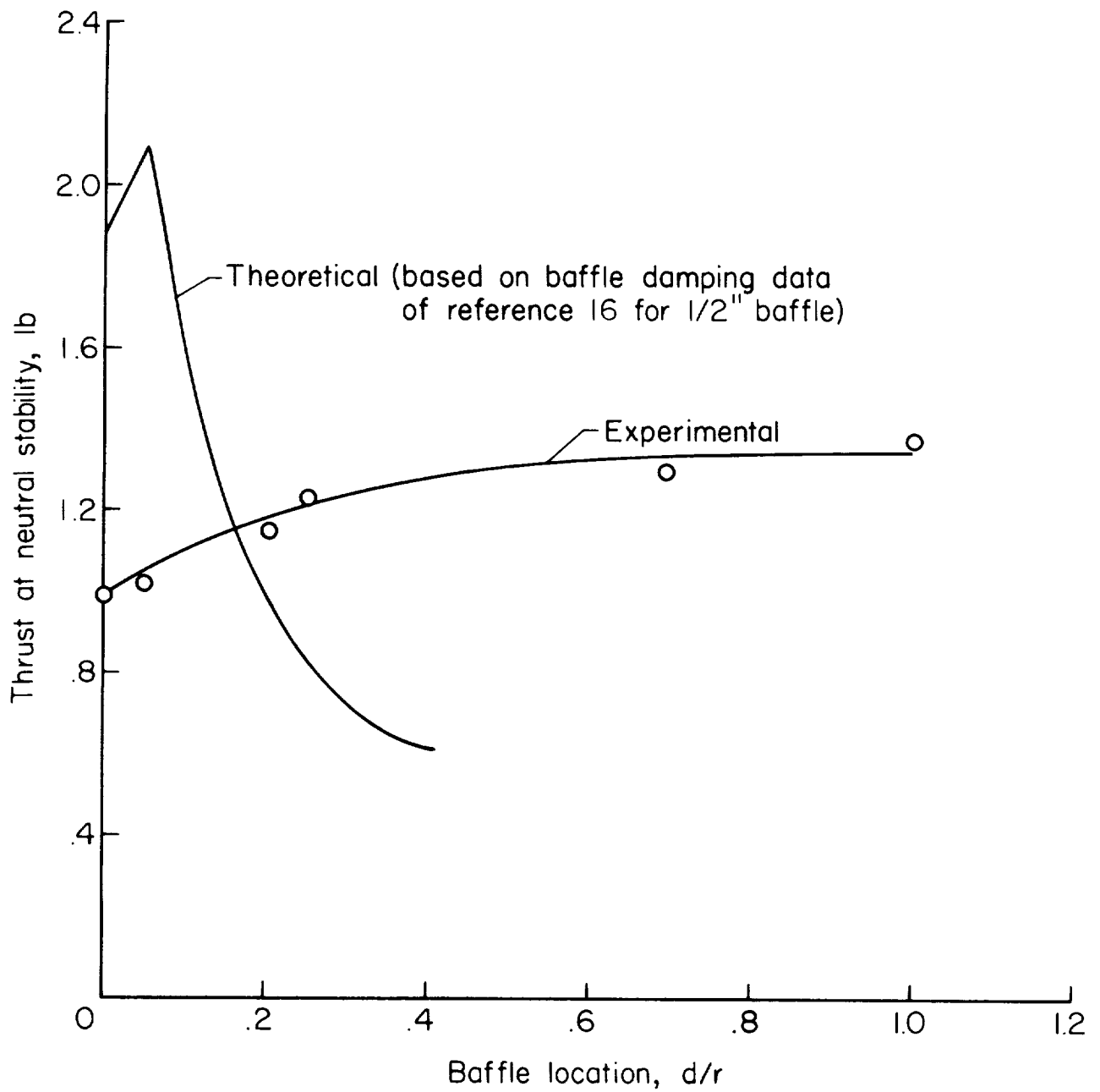
(a) Damping of the fundamental mode as a function of thrust.

Figure 8.- Four-degree-of-freedom analogous system; $K_\alpha = 340$.



(b) Thrust at neutral stability as a function of c_γ .

Figure 8.- Continued.



(c) Thrust at neutral stability as a function of baffle location.

Figure 8.- Concluded.

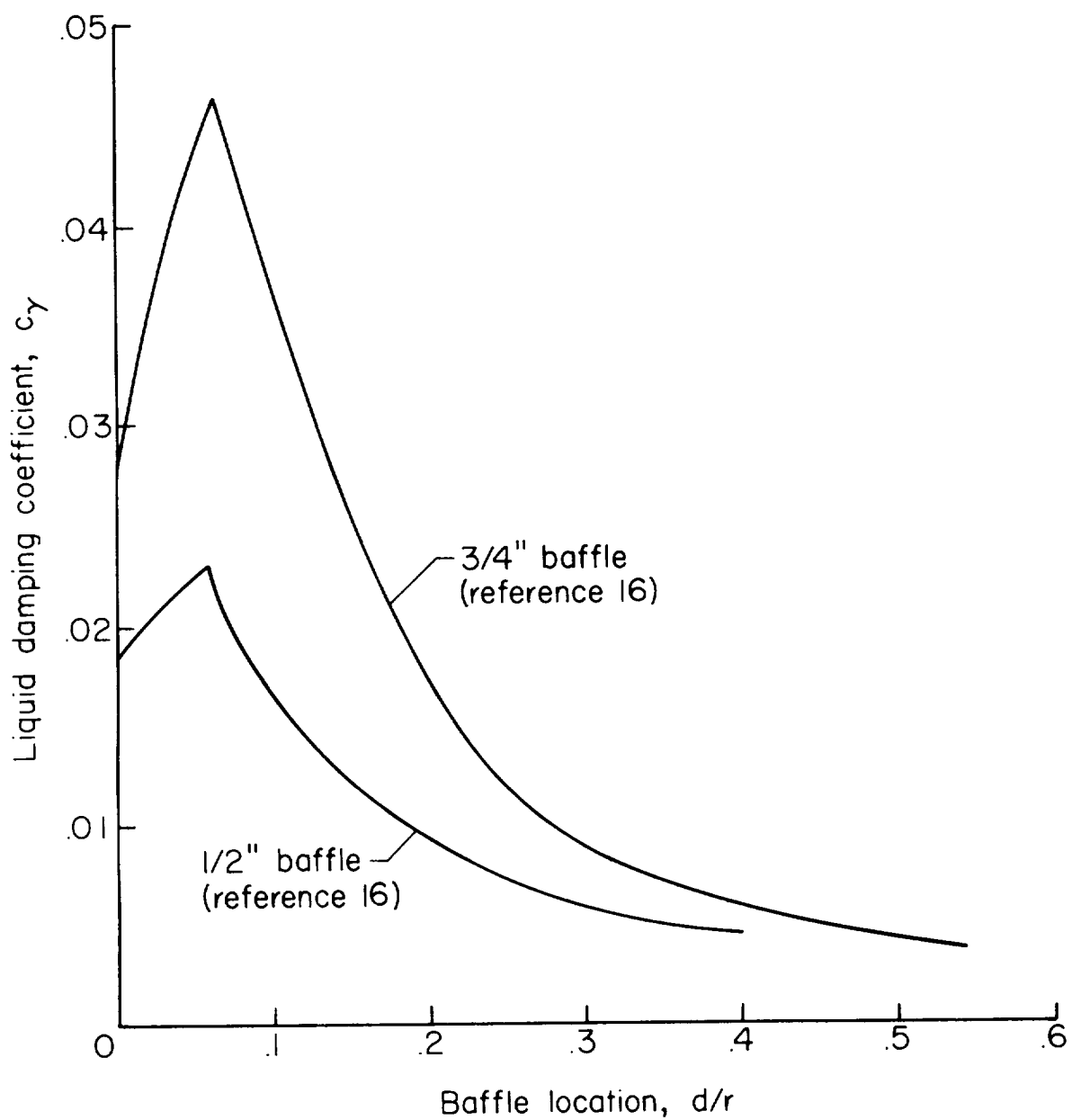


Figure 9.- Variation of liquid damping coefficient with baffle location.

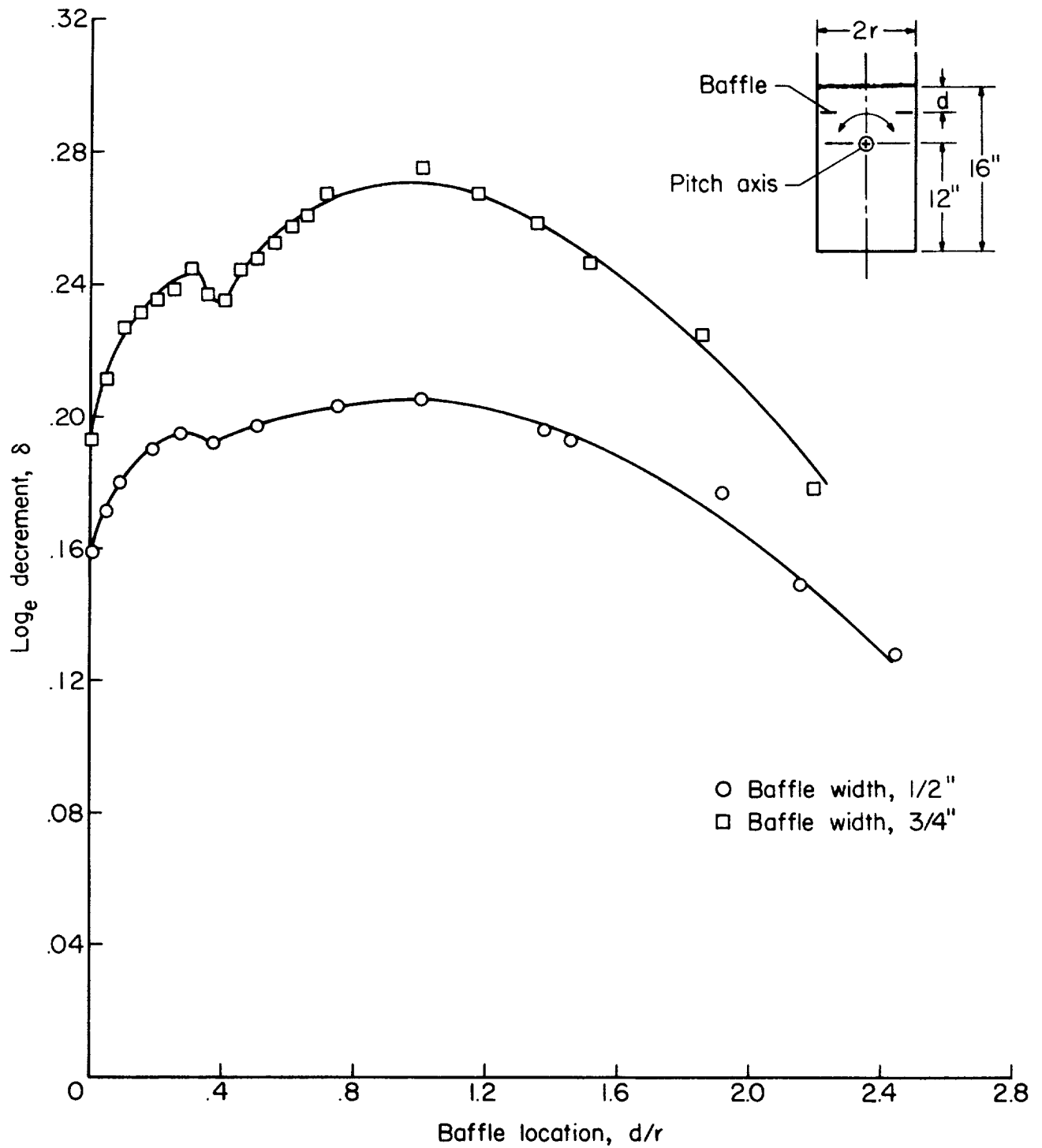


Figure 10.- Variation of δ with baffle location for a fundamental pitching oscillation.

